

## Use Authorization

In presenting this dissertation in partial fulfillment of the requirements for an advanced degree at Idaho State University, I agree that the Library shall make it freely available for inspection. I further state that permission to download and/or print my thesis for scholarly purposes may be granted by the Dean of the Graduate School, Dean of my academic division, or by the University Librarian. It is understood that any copying or publication of this thesis for financial gain shall not be allowed without my written permission.

Signature \_\_\_\_\_

Date \_\_\_\_\_

**Development of an Interior Component Flooding Fragility  
Model and Design of Component Flooding Evaluation  
Laboratory Safety Circuit**

by

**Sneha Suresh**

A thesis

submitted in partial fulfillment

of the requirements for the degree of

Master of Science in the Department of Nuclear Engineering

Idaho State University

Spring 2017

## Committee Approval

To the Graduate Faculty:

The members of the committee appointed to examine the thesis of SNEHA SURESH find it satisfactory and recommend that it be accepted.

---

Dr. Chad Pope,  
Major Advisor

---

Dr. S. Hossein Mousavinezhad  
Committee Member

---

Dr. Bruce Savage  
Graduate Faculty Representative

## **Acknowledgments**

I would like to express my sincere gratitude to Dr. Pope for providing me an opportunity to work under him in the CFEL project. His timely guidance and useful critiques of this research work has been of great help in completion this thesis.

I would also greatly extend my thanks to Dr. Bruce Savage and Dr. S. Hossein Mousavinezhad for their advice and support during the course of this thesis.

I would thank my parents for their never-ending support and encouragement through my master's journey. Last but not the least my sincere thanks Allison and all the other CFEL team members for their help and a few of my close friends for their moral support.

# **Contents**

List of Tables .....	vi
List of Figures .....	vii
List of Abbreviations .....	viii
Abstract.....	x
1. Introduction .....	1
2. Background .....	2
3. Portal Evaluation Tank .....	3
3.1 Design.....	3
3.2 Testing in PET .....	4
2.3 Door Test Data .....	9
4 Fragility Modeling .....	10
4.1 Seismic Modeling .....	11
4.2 Bayesian Analysis .....	13
4.2.1 Bayesian Regression Modeling .....	13
4.2.2 Software Tools .....	14
4.2.3 Bayesian Regression Model Example.....	15
4.3 Flooding Bayesian Analysis .....	22
5.0 Current Work .....	23
5.1 Other OpenBUGS Link Functions .....	26
5.2 Model Selection via DIC .....	28
5.2.1 Exploring Model Fit Using DIC.....	29
5.2.2 DIC Model Analysis for NASA Data .....	30
6.0 CFEL Key Features .....	32
6.1 Safety Circuit Design .....	33
6.1.1 Safety Circuit Implementation .....	38
6.2 Reliability of Components.....	43
6.2.1 Reliability Prediction Definitions.....	43
6.2.2 Bathtub Curve .....	45
6.2.3 R(t) Calculations .....	46
6.2.4 Reliability Block Diagrams .....	47
6.2.5 Fault Tree Analysis .....	50
7 Conclusion.....	53

8 Future Work .....	53
9 Bibliography .....	54
Appendix A.....	55
Appendix B.....	56
Appendix C.....	59
Appendix D.....	63
Appendix E .....	66

## **List of Tables**

Table 1. Door Test Data .....	10
Table 2. O-Ring Thermal Stress Data Prior To Launch of Challenger In January 1986.....	16
Table 3. OpenBUGS Script for Regression Model for the O-ring Fragility Example.....	19
Table 4. Parameter Results (Mean Values) Of the Fragility Regression .....	20
Table 5. Updated PET Door Test Experimental Data .....	23
Table 6. OpenBUGS Script for Depth Model.....	25
Table 7. Results of the Depth Model .....	25
Table 8. Models Responses to Link Function.....	27
Table 9. Errors Observed While Using Different Link Functions.....	27
Table 10. Information on DIC and Other Parameters of the Seven Models.....	30
Table 11. DIC and p-values for the NASA Example Data.....	31
Table 12. Truth Table .....	34

## List of Figures

Figure 1. Portal evaluation tank.....	4
Figure 2. Interior hollow core wooden door.....	5
Figure 3 Results of door test 0. ....	6
Figure 4. Plot of time Vs water height. ....	7
Figure 5. Plot of time Vs the flow rate. ....	7
Figure 6. Plot of time Vs water height for door Test 3 and 4 .....	8
Figure 7. Door test 3 flow information. ....	8
Figure 8. Door test 4 flow information. ....	9
Figure 9. Illustration of seismic fragility model for an example component.....	12
Figure 10. Solid rocket motor cross section shows positions of tang, clevis and O-rings. ....	15
Figure 11. P-value predictability. ....	20
Figure 12. Fragility model curves for the O-ring example. ....	22
Figure 13. Common influencing factors that affect component flooding fragility. ....	23
Figure 14. Testing bay. ....	32
Figure 15. The key features of CFEL.....	33
Figure 16. K-map. ....	36
Figure 17. First safety circuit logic. ....	36
Figure 18. Second Safety Circuit using a 2:1 MUX. ....	37
Figure 19. Online simulation of first safety circuit.....	39
Figure 20. Second safety circuit with 2:1 MUX's internal circuit. ....	40
Figure 21. Online simulation of second safety circuit.....	40
Figure 22. Implementation of first safety circuit on breadboard. ....	41
Figure 23. Implementation of second safety circuit on breadboard. ....	42
Figure 24. Understanding MTBF. ....	44
Figure 25. Typical bathtub curve. ....	46
Figure 26. Components connected in series.....	48
Figure 27. Components connected in parallel. ....	48
Figure 28. RBD for the first safety circuit.....	49
Figure 29. Second safety circuit RBD. ....	50
Figure 30. FT analysis for the first safety circuit. ....	51
Figure 31. FT analysis for the second safety circuit. ....	52



## **List of Abbreviations**

PET	Portal Evaluation Tank
CFEL	Component Flooding Evaluation Laboratory
NPP	Nuclear Power Plant
PRA	Probabilistic Risk Assessment
MERC	Measurement and Control Engineering Research Center
ISU	Idaho State University
DOE	Department of Energy
LWRS	Light Water Reactor Sustainability Program
GPM	Gallons Per Minute
BUGs	Bayesian inference using Gibbs sampling
MCMC	Markov Chain Monte Carlo
GML	General Linearized model
BIC	Bayesian Information Criteria
DIC	Deviance Information Criterion
MUX	Multiplexer
K-map	Karnaugh map
T-T	Truth Table
BCD	Binary Coded Decimal
RTL	Resistor-Transistor Logic
TTL	Transistor-Transistor Logic

DTL	Diode–Transistor Logic
CMOS	Complementary Metal-Oxide-Semiconductor logic
LS	Low power Schottky
TI	Texas Instruments
LED	Light Emitting Diode
FIT	Failure In Time
MTBF	Mean Time Between Failure
FT	Fault Tree
RDB	Reliability Block Diagram
FTA	Fault Tree Analysis

## **Abstract**

The goal of this two-part thesis was to design and develop a flooding fragility model for an interior hollow core wooden door tested in the Portal Evaluation Tank of the Component Flooding Evaluation Laboratory (CFEL) using Bayesian analysis. For the data acquired in the door tests, various models were developed using Bayesian regression modeling. An attempt was also made to select the best model to represent the failure probability. The second section of this thesis focused on safety analysis of the CFEL. Simple yet effective safety circuits using digital control logic was designed and built. Reliability and fault tree analysis was done to verify the correctness of two safety circuits. Based on the reliability analysis results, one operational safety circuit was selected for CFEL.

# 1. Introduction

In Nuclear Power Plant (NPP) Probabilistic Risk Assessment (PRAs) the failure of the components from the flooding phenomenon due to water damage is not elucidated. The March 11, 2011, Tsunami at the Fukushima Daiichi NPP has highlighted the importance of flooding as a potential hazard. Traditionally, NPP flooding analysis involves identification of the frequency of expected flooding depths and then assuming components below the flooding depths fail during the flooding event. However, there is merit in understanding the reliability of NPP components under flooding conditions to allow a more robust evaluation of flooding hazards.

The Component Flooding Evaluation Laboratory (CEFL) research group, is involved in the testing of numerous NPP components such as doors, feed throughs, pipes, electrical and mechanical components. These components are tested to failure under mainly three categories namely the water rise, water spraying and the wave impact flooding events.

Using the data generated from the flooding events, we then develop stochastic models that can later be used to analyze the probabilistic risks associated with respect to component flooding of NPP with the help of a mathematical modeling. These models can then be used to develop flooding fragility curves for the component being tested.

The purpose of this thesis is to understand, develop a fragility model for the mechanical component, an interior hollow core wooden door tested in CFEL, and building of a safety circuit for a secure and controlled operation in CFEL.

## 2. Background

Flooding has always been a potential risk to NPP as they are typically located near the oceans or other bodies of water. Studies were done in CFEL research group on numerous flooding accidents that have occurred over the years [1]. Shockingly there have been 18 accidents at NPPs in the USA alone. Common reasons include leakage from containment pipe ruptures, failure of seals, loss of off-site power causing the emergency core cooling system to be flooded. This is a stark reminder for the need of deeper understanding of NPP component reliability under flooding. Thus, the need and construction of CFEL was well established.

The construction of CFEL is underway in the Measurement and Control Engineering Research Center (MERC) building at Idaho State University (ISU). This project is funded by the Department of Energy (DOE) under the Light Water Reactor Sustainability Program (LWRS). This project began with the design and construction of small-scale experiments for a better understanding of the behavior of the mechanical and electrical components under flooding conditions. Components such as radios, laptops, small scale doors were tested [2]. Using the information obtained, the need of flooding fragility curves in a NPP risk analysis were established. A flooding fragility curve is a plot of the probability of failure of a defense as a function of a load event. The loading event maybe caused due to temperature, pressure, depth of water etc.

Full-scale experiments commenced in a tank constructed specifically to conduct large-scale experiments, called the Portal Evaluation tank or PET. The next section discusses the design and the full-scale experiments conducted in PET.

## **3. Portal Evaluation Tank**

### **3.1 Design**

The PET is a crucial part of CFEL where component testing takes place (Figure 1). A brief description of PET follows. The PET is a semi-cylindrical steel tank with 7,500 liter capacity with a 2.4 x 2.4 m opening for various installations such as doors, pipes, feedthroughs and other components. It has two 7.5 cm inlets on the side with a single 5 cm outlet at the bottom. It also has four outlets at the top for pressure and air relief valves, a pressure gauge and a pressure transducer. A 5 Hp submersible pump is connected to the PET using a 3 inch PVC pipe. The pump will take about 20 minutes to fill the tank at the flow rate of 100 GPM for 3-inch pipe. If the pump is turned on in full power, a flow rate of about 300 GPM could be achieved, which takes about 8 minutes to fill the tank. The pump is located inside a 30,000-liter water reservoir. For the measurement of flow, leakage rate and water depth an electronic flow meter, ultrasonic sensor and a pressure transducer is used [3].



**Figure 1. Portal evaluation tank.**

### **3.2 Testing in PET**

Hollow core interior wooden door experiment was the first successful full scale testing done in PET shown in Figure 2. These doors were subjected to a water rise scenarios. For the initial set of experiments, a hollow core wooden door of dimensions 3-feet wide and 7-feet tall was chosen. The door was hung onto the tank with the help of the door frame and wall [3].



**Figure 2. Interior hollow core wooden door.**

Once the construction of the wall assembly was done, it was then installed in the PET. To prevent leakage, silicone and insulating foam were applied. The general experimental approach was to fill the PET with water under the door failed at a certain height. The aim was to observe door failure modes.

A set of five full scale door experiments were conducted for a span of two months [3]. In all the five experiments the depth in inches, a flow rate in gal/min and temperature in Fahrenheit were measured. Summary of the tests is discussed below.



The first experiment was conducted on June 27, 2016. Failure occurred at a water depth of 21 inches at approximately 11.50 A.M. The door swung open when the wooden section of the latch engagement area failed. Here, no damage to the door occurred but damage to the wooden piece on the door frame was visible. The results of door test 0 as shown in Figure 3.

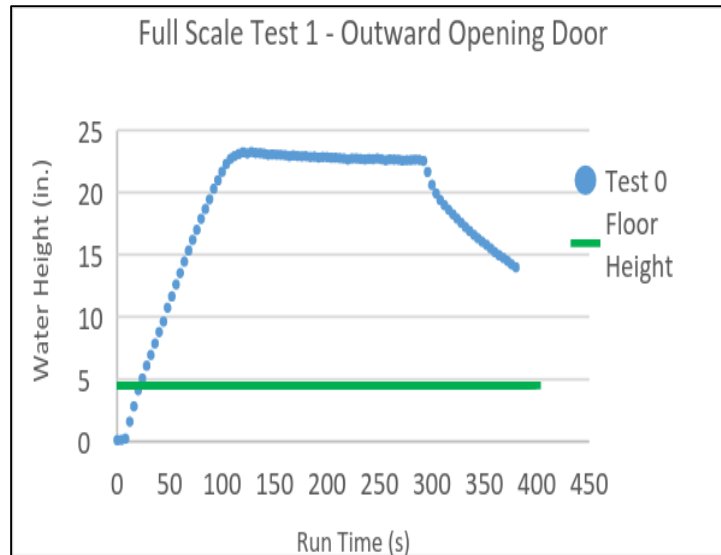


**Figure 3 Results of door test 0.**

The second experiment immediately followed the first one. Minor changes were done to conduct this experiment. The broken latch section of the wooden door was glued back in place and the metal bracket was installed. To prevent the excessive leakage as recognized from the first experiment, a plywood strap was attached at the bottom of the door and was secured by the studs around the door frame. The pump was turned on at 12:28 P.M. The observed flow rate was 294 gpm and it filled the tank in 10 mins with no leakage. The water level inside the tank reached about 40 inches within 3 minutes. The results of door test 1 and 2 are shown in Figure 4 and Figure 5.

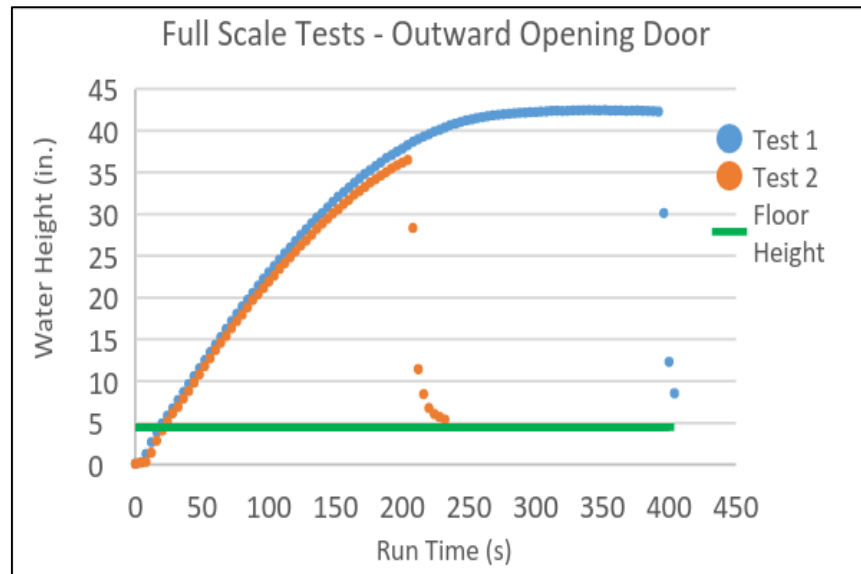


**Figure 4. Plot of time Vs water height.**

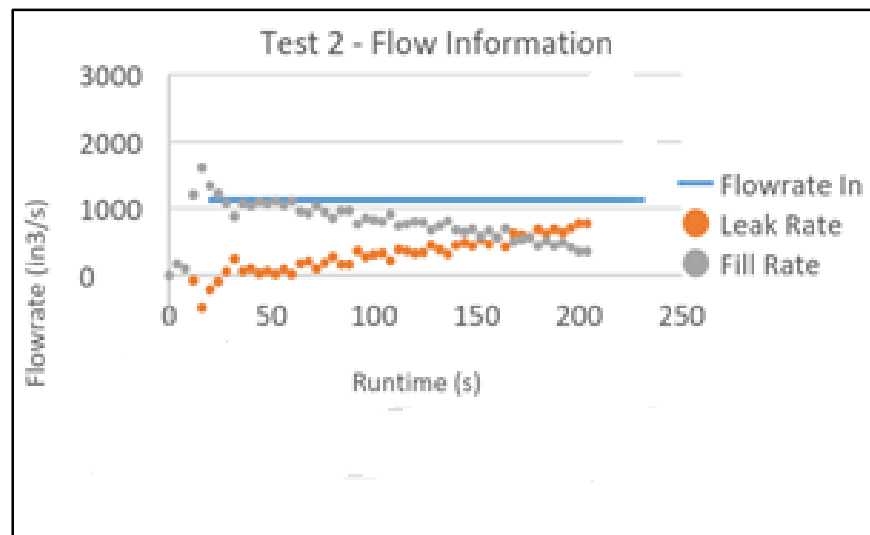


**Figure 5. Plot of time Vs the flow rate.**

The following tests involved the inward opening of the doors. Since the water inside the tank would help to force the door against its frame, a reduction in the water leakage rate was anticipated. The results of the tests are shown below in Figure 6, Figure 7 and Figure 8.

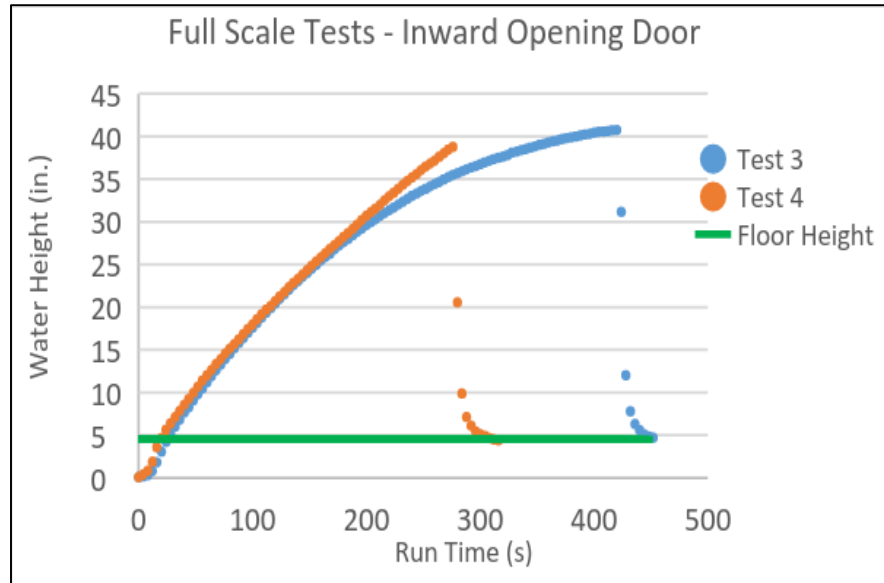


**Figure 6. Plot of time Vs water height for door Test 3 and 4**

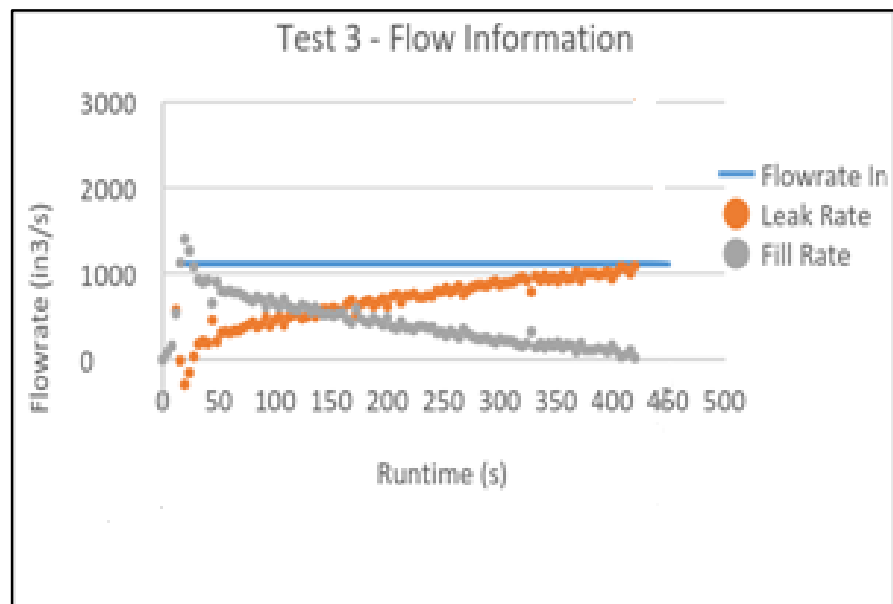


**Figure 7. Door test 3 flow information.**

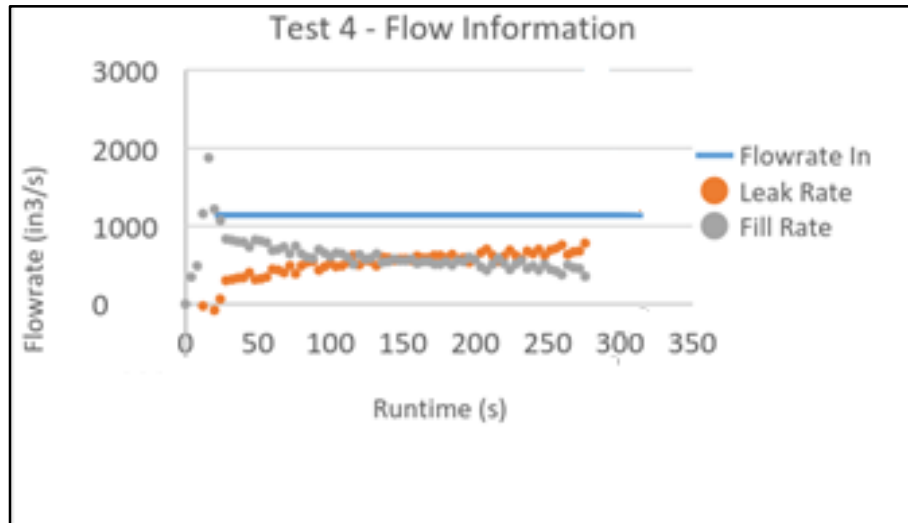


**Figure 8. Door test 4 flow information.**

In the plots featuring the flow rate, it is observed that leakage rate becomes negative at the beginning of the test. This is attributed to rapid water level changes in a specific area above the instrumentation and the assumptions were made to simplify the data analysis [3].

## 2.3 Door Test Data

For each of the different door tests done on a particular day, data was collected for height, flow rate and temperature was collected and condensed in a table as shown Table 1.

The test column indicates the date the door test was performed along with the test number. The next column indicates the greatest depth in inches at which the door failed. Next is the flow rate in gal/min, this was calculated as the average of flow rate data collected for a door test number. Lastly, the temperature in Fahrenheit was also

calculated as the average for the specific door test. Failure (1) for a test was decided when the damage to the door was permanent. Success (0) was defined when an equilibrium state was reached between leakage and flow rate. The data in the table will be converted in eight full sets for modeling.

**Table 1. Door Test Data**

<i><b>Test Dates</b></i>	<i><b>Depth(in)</b></i>	<i><b>Flow Rate(gal/min)</b></i>	<i><b>Temp(F)</b></i>	<i><b>Failure</b></i>
06-24-2016	11.54	NA	65.59	0
06-24-2016	NA	291	NA	0
06-24-2016	23.23	291.5	65.98	0
06-27-2016	20.75	292.5	67.04	0
06-27-2016	42.3	292.5	66.02	1
07-20-2016	21.05	297	67.67	0
07-20-2016	24.22	294.5	66.60	0
07-20-2016	35.41	292.5	66.87	1
08-20-2016	40.76	291	68.33	1
08-20-2016	38.85	294	68.14	1

## 4 Fragility Modeling

Door tests data obtained from the full-scale interior door testing are now fit into a mathematical model. There are two factors of concern while approaching this method. Firstly, what parameters needs to be considered like water height, flow rate, leakage rate etc. Secondly, what kind of probability distribution can be used to model the failure. This thesis began with the investigation of various mathematical models to model the obtained flooding data from the full-scale door test. The approach to use the obtained flooding experiment data is by use of fragility models.

## 4.1 Seismic Modeling

Traditionally, fragility models have been used in the NPP industry by the seismic community to determine the failure probability of a component or structure. Fragility is the conditional probability of "failure" of a structure or component for a given peak ground acceleration. This thesis began with investigating the possibility of adapting seismic modeling. Seismic fragility defines the probability of a certain failure mode as:

$$P_f(A) = \Phi \left( \frac{\ln \left( \frac{A}{A_m} \right)}{\beta_R} \right) \quad (1)$$

Where  $A$  is the peak ground acceleration,  $A_m$  is the median ground acceleration,  $\Phi$  is the standard Gaussian cumulative distribution function, and  $\beta_R$  is the log standard deviation of randomness. For a given failure state, a curve can then be generated where the probability of failure is a function of the peak ground acceleration. Seismic fragilities are a distribution of the peak ground acceleration at which the component will fail [2]. A single variable ground acceleration ( $g$ ) as a function of earthquake levels is used to represent the component or structure failure as a simple monotonically-increasing fragility curve. The probability of a component failing (or reaching a specified damage state) is described as a random variable governed by an underlying probability distribution (Figure 9).

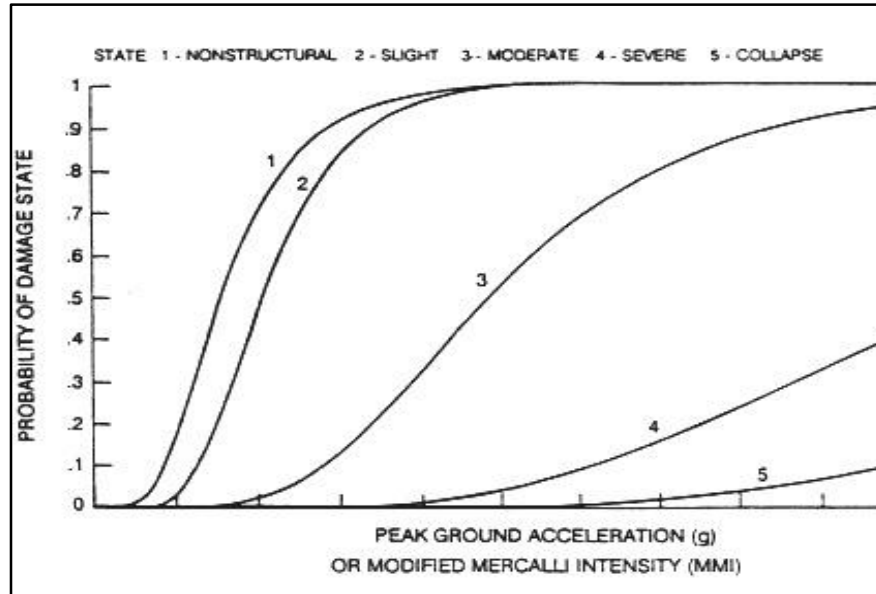


**Figure 9. Illustration of seismic fragility model for an example component**

It was observed that for some flooding types such as submersion or slow-rise flooding, a simple 1-Dimensional fragility model may be sufficient. This was demonstrated in Dave Kamerman's thesis for the small-scale component testing experiment conducted by the CFEL research group [2]. However, a thorough understanding of the seismic modeling determined the variance of flooding method from the seismic fragility evaluation. One of the main reasons was the fact that seismic fragility modeling considered a single parameter i.e. the peak ground acceleration to characterize the probability of failure of a component. However in reality, other flooding types like waves or spray events require more observables to develop a fragility model.

## 4.2 Bayesian Analysis

Expanding on seismic modeling, it may be observed that for a more detailed and better characterization of failure, other parameters such as, X, Y and Z parts of ground motion, age of the component, frequency of the wave, anchorages and specifics of the component or any of the above combination. Overcoming the limitations of seismic modeling requires more observables instead of a single “driven” parameter. So, for fragility modeling a more flexible and data informed approach i.e. Bayesian fragility modeling through phenomena driven regression modeling is used.

### 4.2.1 Bayesian Regression Modeling

In probability theory Bayes theorem [4] is given by equation 2

$$P(H|D) = P(H) \frac{P(D|H)}{P(D)} \quad (2)$$

Where,

$P(H|D)$  : Posterior distribution, which is conditional upon the data D that is known related to the hypothesis H

$P(H)$  : Prior distribution, from knowledge of the hypothesis H that is independent of data D

$P(D|H)$  : Likelihood, or aleatory model, representing the process or mechanism that provides data D

$P(D)$ : Marginal distribution, which serves as a normalization constant



One of the applications of Bayes theorem is Bayesian inference. In Bayesian regression modeling, the aim is to build an aleatory model to obtain association or connection between parameters (H) and observables (D) and use them to calculate the posterior probability. An aleatory model pertains to stochastic or non-deterministic events, the outcome of which is described using probability.

The Bayesian method has several attributes. It can be applied to any probability distribution and calculate the predicted distribution of unobserved data used for model checking where non-significant variable can be eliminated. It also allows for the flexibility in adjusting the model to better reproduce the observed data and uncertainties in observable parameters.

#### **4.2.2 Software Tools**

The most common software tool used for Bayesian analysis is the Bayesian inference using Gibbs sampling, commonly called as the BUGs. BUGs is a software package for performing Bayesian inference using Markov Chain Monte Carlo (MCMC) which is based on Gibbs sampling. Two popular tools from the BUGS family that use MCMC sampling are WinBUGS and OpenBUGS. Both software packages are freely available online. Advantages of OpenBUGS over WinBUGS is, the former is open source, has greater flexibility, and extensibility. Also, a user selected node can be updated after every compilation. OpenBUGS supports over 20 distributions. Discrete and continuous univariate and multivariate are some of the supported distributions. It also offers support for some of the most common and frequently used distributions in PRA such as Binomial, Poisson, Exponential, Weibull, Gamma, Beta, Lognormal and Uniform [4].

### 4.2.3 Bayesian Regression Model Example

Taken directly from the reference [1], the example given below elucidates the Bayesian regression modeling. This example will be used as a reference modeling for the flooding data obtained from the door tests. The script used to model the O-ring example is modified accordingly for the flooding data. The example data is taken from the NASA Space Shuttle program-related to O-ring impacts. Each shuttle had three primary and three secondary O-rings [5]. The O-ring was a circular gasket designed to separate the sections of the rocket booster between each fuel segment. The location of O-rings is shown in Figure 10. Appendix A shows the O-ring location in detail.

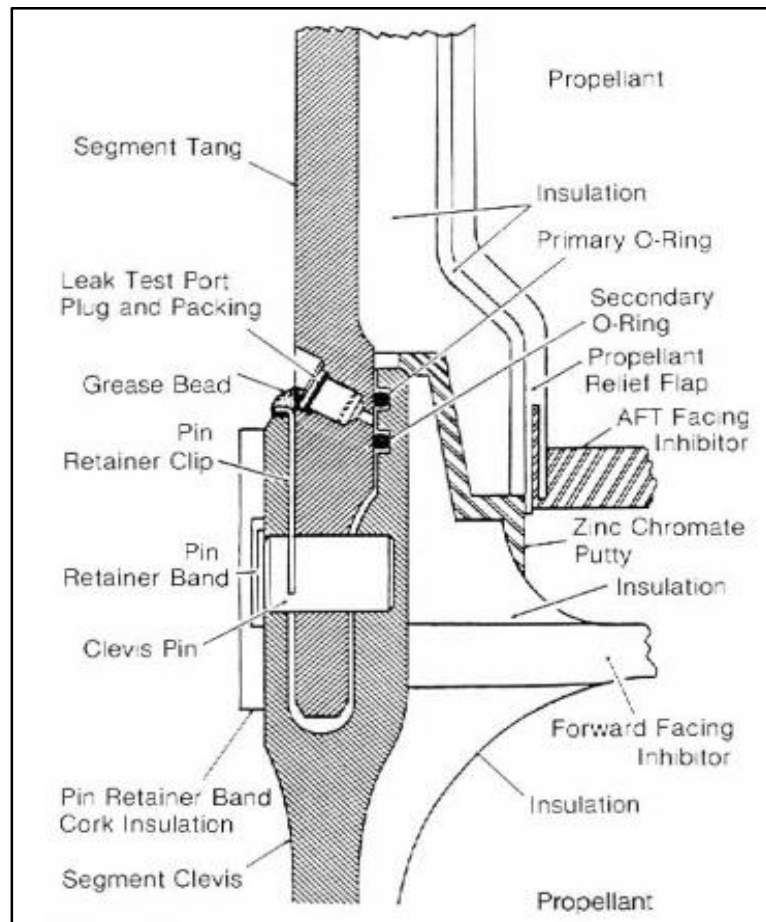


**Figure 10. Solid rocket motor cross section shows positions of tang, clevis and O-rings.**

Table 2 shows the data related to the O-ring impact. The column labeled “distress” represents erosion or blow-by of an O-ring.

**Table 2. O-Ring Thermal Stress Data Prior To Launch of Challenger In January 1986**

<i>Flight</i>	<i>Distress</i>	<i>Temperature (°F.)</i>	<i>Pressure (psig)</i>
1	0	66	50
2	1	70	50
3	0	69	50
5	0	68	50
6	0	67	50
7	0	72	50
8	0	73	100
9	0	70	100
41-B	1	57	200
41-C	1	63	200
41-D	1	70	200
41-G	0	78	200
51-A	0	67	200
51-C	2	53	200
51-D	0	67	200
51-B	0	75	200
51-G	0	70	200
51-F	0	81	200
51-I	0	76	200
51-J	0	79	200
61-A	2	75	200
61-B	0	76	200
61-C	1	58	200

To perform the model analysis, two things are required. First, the need of a model that represents the failure of an O-ring during the launch of the spacecraft. Second, the key variable associated with binomial modeling is the failure on demand,  $p$ . However, it

is necessary to determine what observable or observables determine the failure for fragility modeling purposes. So, it may lead to turning the parameter  $p$  into its own model.

A very commonly used failure on demand model is the binomial model. In simple words, a change of state in a parameter occurs in response to a demand. The binomial model is under a broad class of model referred to as the General Linearized Models (GLMs). It is a conventional linear regression model for a continuous response variable given continuous and/or categorical predictors [6].

There are three components to any GLM:

1. *Random Component* – refers to the probability distribution of the response variable ( $Y$ ); e.g. normal distribution for  $Y$  in the linear regression, or binomial distribution for  $Y$  in the binary logistic regression. Also, called a noise model or error model.
2. *Systematic Component* - specifies the explanatory variables ( $X_1, X_2, \dots X_k$ ) in the model, more specifically their linear combination in creating the so-called linear predictor; e.g.,  $\beta_0 + \beta_1 X_1 + \beta_2 X_2$ .
3. *Link Function,  $\eta$  or  $g(\mu)$*  - specifies the link between random and systematic components. It says how the expected value of the response relates to the linear predictor of explanatory variables; e.g.,  $\eta = g(E(Y_i)) = E(Y_i)$  for linear regression, or  $\eta = \text{logit}(\pi)$  for logistic regression [6].

For Binary Logistic Regression model, the binary response variable  $Y$  depends on a set of  $k$  explanatory variables,  $X=(X_1, X_2, \dots X_k)$ .

$$\text{logit}(\pi) = \ln \left( \frac{\pi}{1-\pi} \right) = \beta_0 + \beta x_i + \dots + \beta_0 + \beta x_k \quad (3)$$

So for the above example, the primary failure model is binomial with parameters  $p$  and  $n$  equal to 6 as there are six affected-rings in the shuttle. In this model,  $p$  is possibly a function of both temperature and applied pressure. One complication with the binomial model is that the parameter  $p$  must be restricted between 0 and 1 since it represents a probability (here the value of  $p$  was 6 and to use logit function it must be restricted between 0 and 1). A common approach to constrain this is to use the logit function for  $p$  and using equation 3,

$$\text{logit}(p) = \ln \left( \frac{p}{1-p} \right) \quad (4)$$

These possibilities are looked in the fragility modeling of this case:

1. Both temperature and pressure drives parameter  $p$  to failure.
2. Temperature alone drives parameter  $p$  to failure.
3. Pressure alone drives  $p$  to failure.

The above cases can be modeled as:

$$\text{logit}(p) = a + bT + cP \quad (5)$$

$$\text{logit}(p) = a + bT \quad (6)$$

$$\text{logit}(p) = a + cP \quad (7)$$

This example problem is now solved for the equations shown above to obtain the value of co-efficients of depth, flow and temperature namely  $a$ ,  $b$ ,  $c$  using OpenBUGS. The

script depicting equation (5) including both temperature and pressure is shown in below in Table 3. A brief description of the script follows, since the model is binomial, binomial distribution is chosen to represent the failure states and next equation (5) is modeled. Diffuse priors are used to model the parameters and any additional information about these parameters if available, can be included too by modifying equations 5, 6 and 7 accordingly. A diffuse prior is a predicted or a vague value that is used to obtained new formation. Lastly, the data from the Table 2 is written in a list form and the script for calculation of  $p$ ,  $a$ ,  $b$  and  $c$  is written inside a for-loop. Other fragility models, equation (6) and equation (7) can be solved by modifying the script for  $\text{logit}(p)$  line.

**Table 3. OpenBUGS Script for Regression Model for the O-ring Fragility Example**

```

model {
for(i in 1:K) {
    distress[i] ~ dbin(p[i], 6)           #binomial distribution
    logit(p[i]) <- a + b*temp[i] + c*press[i] #model with temperature and pressure
}
# Prior distributions and the parameters (diffuse priors)
a ~ dnorm(0, 0.000001)
b ~ dnorm(0, 0.000001)
c ~ dnorm(0, 0.000001)
}
data
list(
    distress=c(0,1,0,0,0,0,0,0,1,1,1,0,0,2,0,0,0,0,0,2,0,1),
    temp=c(66,70,69,68,67,72,73,70,57,63,70,78,67,53,67,75,70,81,76,79,75,76,58),
    press=c(50,50,50,50,50,50,100,100,200,200,200,200,200,200,200,200,200,200,200,200,200,200,200),
    K=23
)

```

The results of running the script are shown in Table 4.

**Table 4. Parameter Results (Mean Values) Of the Fragility Regression Models for the O-Ring Case**

<i>Parameter</i>	<i>Equation 5</i>	<i>Equation 6</i>	<i>Equation 7</i>
<i>a</i> (intercept)	2.1	5.2	-5.0
<i>b</i> (temperature coefficient)	-0.10	-0.12	n/a
<i>c</i> (pressure coefficient)	0.012	n/a	0.013
Bayesian P-value	0.19	0.21	0.26

In Table 4, mean values are obtained for the applicable parameters in the logistic regression fragility models from OpenBUGS. Bayesian P-value is also obtained for each model. This P-value metric can be used to determine model validity. Closer the value of P to 0.5 higher the predictive capability (Figure 11). So, equation 7 (only a function of pressure) is a slightly better model than the other two. However, since there is just a slight variation in the P-values for the three model, two conclusions are drawn. One, a simple binominal model is adequate. Two, if additional flexibility is afforded in case additional data is collected, the model with both pressure and temperature i.e. equation (5) may be selected.

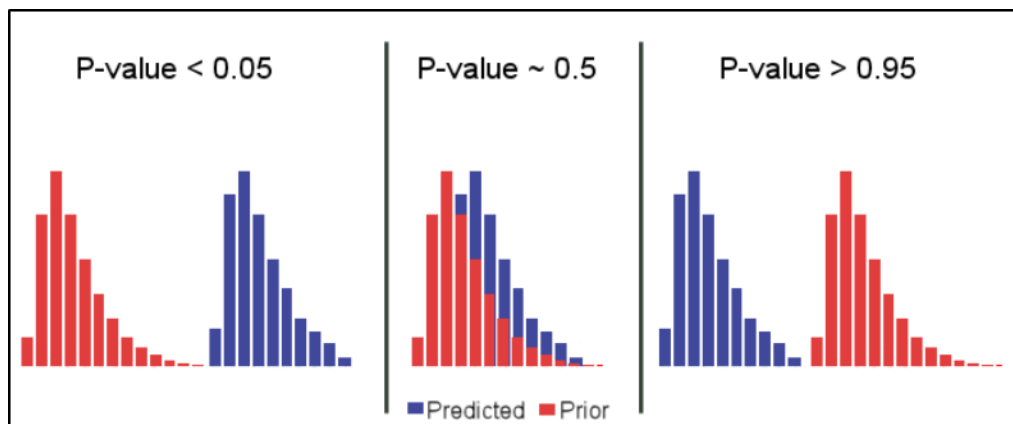


**Figure 11. P-value predictability.**

The parameters from table 2 can then be used with fragility model to calculate the failure probability  $p$  for an O-ring as a function of pressure and temperature. Using equation (5) fragility model, we can determine the p-value and the derivation is shown below,

$$\text{logit}(p) = \ln\left(\frac{p}{1-p}\right) = a+bT+cP$$

$$\frac{p}{1-p} = e^{a+bT+cP}$$

$$p = (1-p) (e^{a+bT+cP})$$

$$p = e^{a+bT+cP} - p(e^{a+bT+cP})$$

grouping p terms together,

$$p (1 + e^{a+bT+cP}) = e^{a+bT+cP}$$

therefore,

$$p = \frac{e^{a+bT+cP}}{1 + e^{a+bT+cP}}$$

multiplying and dividing the above equation by  $e^{a+bT+cP}$

$$p = \frac{1}{e^{-(a+bT+cP)} + 1} \quad \left[\frac{1}{e} = e^{-1}\right]$$

Hence, the p value is calculated using the equation

$$p = \frac{1}{e^{-(a+bT+cP)} + 1} \quad (8)$$

Plotting the three fragility models provides the results shown in Figure 12. It is a plot of the temperature vs the failure probability,  $p$ . The fragility model given by Equation 7 is invariant to any temperature changes ( $p$  stays at 0.024) since the temperature parameter is removed from the regression model for that particular case.



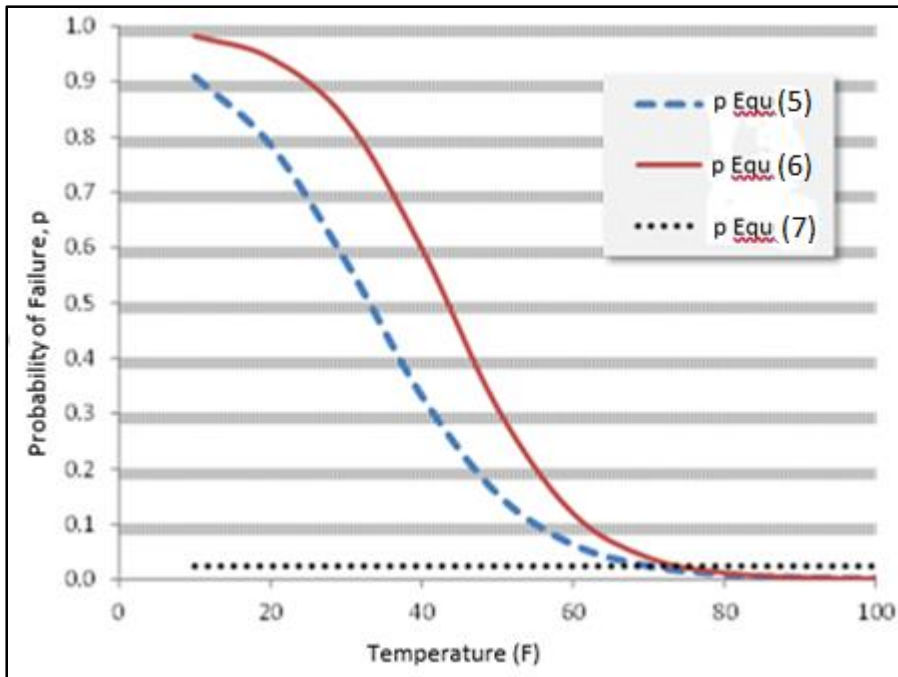


Figure 12. Fragility model curves for the O-ring example.

### 4.3 Flooding Bayesian Analysis

This section talks about how the above example can be used as a reference for the flooding data obtained from the door tests. As discussed in section 4.2, one of the complications in flooding fragility modeling is the involvement of “many” factors contribution to the failure modeling instead of a single factor. Common observables include age, inundation level, pressure, mass, temperature, component type (Figure 13). Some thinking must be given as to what factors would be most important for regression modeling. Nonetheless, an advantage of using Bayesian quantification approach is parameters in the regression model that have no significant role are found to be negligible. This behavior is outlined in the next section with the available door test data conducted in PET.

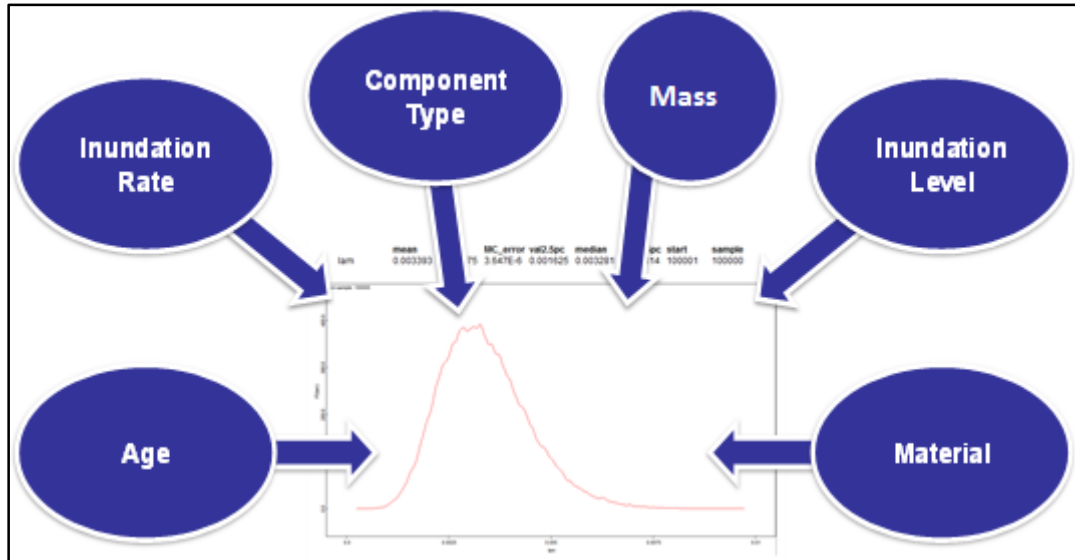


Figure 13. Common influencing factors that affect component flooding fragility.

## 5.0 Current Work

The recent experiment conducted in the PET was the full-scale door tests. The instrumentation fitted on PET recorded water depth (D), flow rate (F) and temperature (T). The experimentation results available was recorded as in Table 1 and was updated for eight completed sets of data as shown in Table 5.

Table 5. Updated PET Door Test Experimental Data

<i>Depth(in)</i>	<i>Flow Rate(gal/min)</i>	<i>Temp(F)</i>	<i>Failure</i>
23.23	291.5	65.98	0
20.75	292.5	67.04	0
42.3	292.5	66.02	1
21.05	297	67.67	0
24.22	294.5	66.60	0
35.41	292.5	66.87	1
40.76	291	68.33	1
38.85	294	68.14	1

Applying a similar analogy of the example problem section, an assumption that depth, flow and temperature may be the parameters that affect the flooding fragility model in this case. The primary model will be the binomial model with parameters  $p$  and  $n=1$  (only one door is potentially challenged during testing). In this model,  $p$  is a possible function of depth, flow and temperature. Following on the lines of the example problem, the parameter  $p$  is constrained between 0 and 1 and logit relation is used for  $p$  (equation 4).

The fragility model in this case will look at 7 possibilities with each of the parameters alone driving the model to failure, combination of two factors and combination of all the three. These models are:

$$\text{logit}(p) = \text{intercept} + aD + bF + cT \quad (9)$$

$$\text{logit}(p) = \text{intercept} + aD \quad (10)$$

$$\text{logit}(p) = \text{intercept} + bF \quad (11)$$

$$\text{logit}(p) = \text{intercept} + cT \quad (12)$$

$$\text{logit}(p) = \text{intercept} + aD + bF \quad (13)$$

$$\text{logit}(p) = \text{intercept} + aD + cT \quad (14)$$

$$\text{logit}(p) = \text{intercept} + bF + cT \quad (15)$$

A script similar to Table 3 was written for the above seven equations. Since there was no predictive capability on temperature and flow the model had to be reduced to the depth variable when  $\text{logit}(p)$  function was used. This script is shown in Table 6. The remaining equations are modelled in the Appendix B.

**Table 6. OpenBUGS Script for Depth Model**

```
#Depth (D) Model
model {
  for(i in 1:tests) {
    failure[i] ~ dbin(p[i], num.tested)
    # Regression model
    cloglog(p[i]) <- int + a*depth[i]
    #failure.rep[i] ~ dbin(p[i], num.tested) # Replicate values for model validation
    #diff.obs[i] <- pow(failure[i] - num.tested*p[i], 2)/(num.tested*p[i]*(1-p[i]))
    #diff.rep[i] <- pow(failure.rep[i] - num.tested*p[i], 2)/(num.tested*p[i]*(1-p[i]))
  }
  #chisq.obs <- sum(diff.obs[])
  #chisq.rep <- sum(diff.rep[])
  #p.value <- step(chisq.rep - chisq.obs)
  # Prior distributions
  int ~ dnorm(0, 0.0001)
  a ~ dnorm(0, 0.001)
}
data
list(num.tested=1, tests=8, depth = c(23.23,20.75,42.3,21.05,24.22,35.41,40.76,38.85), failure =
c(0,0,1,0,0,1,1,1))
inits
list(int=0, a=0)
```

The results of running the script in Table 6 give the depth coefficient and the intercept value shown in Table 7. The Bayesian p-value is not available because the number of samples obtained was less and hence the mean p-value was not obtained but currently work is being done on this part.

**Table 7. Results of the Depth Model**

<i>Parameter</i>	<i>Mean Value</i>
intercept	3.827
a (depth coefficient)	-110.2
Bayesian p-value	—

Since no conclusive results was obtained by using the logit function, the next section deals with possible functions that could potentially replace logit. Once the necessary coefficient values are established, equation (9) would be re-modelled for this case as:

$$p = \frac{1}{e^{-(intercept+aD+bF+cT)}+1} \quad (16)$$

## 5.1 Other OpenBUGS Link Functions

The shortcoming with the logit function was recognized and an attempt was made to check other available link functions that could provide complete results for equations 9-15. The available link functions that are supported by OpenBUGS are log, logit, cloglog and probit [7]. They are defined as:

$$\log(p): \text{natural logarithm of } p \quad (17)$$

$$\text{logit}(p) = \ln\left(\frac{p}{1-p}\right) \quad (18)$$

$$\text{cloglog}(p): \text{complementary log log of } p \ln(-\ln(1-p)) \quad (19)$$

$$\text{probit}(p): \text{inverse of standard normal cdf } \phi(p) \quad (20)$$

Table 8 shows link functions behavior with designed flooding fragility models.

**Table 8. Models Responses to Link Function**

	<i>variables</i>	<i>log</i>	<i>logit</i>	<i>cloglog</i>	<i>probit</i>
1	flow rate	•	✓	✓	❖
2	depth	•	✓	✓	❖
3	temperature	✓	✓	✓	❖
4	flow rate, depth	•	○	✓	❖
5	flow rate, temperature	•	✓	✓	❖
6	depth, temperature	•	○	✓	❖
7	flow rate, depth, temperature	•	○	✓	❖

As seen, only the models with ✓ indicate the complete results are available for intercept and coefficients. The symbols used in the table represents the errors faced while compilation and they are listed below in Table 9.

**Table 9. Errors Observed While Using Different Link Functions**

<i>Symbols</i>	<i>Observed Errors</i>
•	Something went wrong in procedure; updater delayed. Sample in module updater.
○	Something went wrong in procedure. Sample in module update rejection.
❖	Something went wrong in procedure node. Value in module graph probit.

Link function cloglog was chosen instead of logit, as it works well with the seven models. This was mainly done to obtain the value of intercepts and mean values of coefficients. These values were then compared with the other seven models to select the best fit. The next step was running the scripts again with cloglog function and calculating the Deviance Information Criterion (DIC) for the selection of a best fit. This will be discussed in the next section. Appendix C has the complete results with mean, standard deviation and other important stats for the seven models updated with cloglog function.

## **5.2 Model Selection via DIC**

Another way to predict the best model fit when the p-value is unavailable is using information criteria. This criteria measure the relative fit. A best model from the relative point of view maybe not very good from an absolute point of view. So, for an absolute model adequacy assessment, it is necessary to examine Bayesian P-value and replicated times [4]. Two commonly discussed information criteria are the Bayesian Information Criteria (BIC) and DIC. DIC is a measure of model fit that can be applied to Bayesian models and that works when the parameter estimation is done using numerical techniques, such as Gibbs samplers. It is particularly useful in Bayesian model selection problems where the posterior distributions of the models have been obtained by MCMC simulation. DIC is a popular Bayesian analog of BIC. DIC has been recommended for selecting among the hierarchical models. A hierarchical model also sometimes called multilevel model has mutual dependence on the selected parameters that affect the modeling [8]. The door test data shows clear interdependence on the factors that have been selected to affect regression modeling as seen in the current work section.

In OpenBUGS, Dbar is automatically monitored by the node called deviance and it requires no additional scripting. But mathematically DIC is calculated as the sum of Dbar and pD [9]

$$\text{DIC} = \text{Dbar} + \text{pD} \quad (21)$$

$$\text{pD} = \text{Dbar} - \text{Dhat} \quad (22)$$

Where,

pD is the effective number of parameters

Dhat is deviance evaluated at posterior mean of parameter(s)

DIC and even pD can be negative in some cases. DIC is usually negative when the density function  $> 1$ . However, if pD turns out to be negative, DIC cannot be used. As a rule of thumb, the model with the smallest DIC usually indicates the best fitting model. For example, consider four models with DICs -11.5, -26, 10, 56. The second model is the best fit model because it has the smallest DIC among the others. It must also be noted that since DIC is a measure of relative fit, a model with the smallest DIC can still be a poor fit [5].

### **5.2.1 Exploring Model Fit Using DIC**

This section deals with DIC application on the flooding data obtained from door test. The scripts are re-written to change the link function from logit to cloglog. First, the seven models are run for 100,000 samples. Next, DIC is selected from the inference menu



of OpenBUGS. DIC now needs to be set and the models are run for another 100,000 more updates. Now the deviance information is collected. Table 10 shows the results obtained from running 100,000 samples and skipping the first 1000 samples.

**Table 10. Information on DIC and Other Parameters of the Seven Models**

<i>Parameter</i>	<i>Equ. 9</i>	<i>Equ. 10</i>	<i>Equ. 11</i>	<i>Equ. 12</i>	<i>Equ. 13</i>	<i>Equ. 14</i>	<i>Equ. 15</i>
Intercept	5.653	-108.0	3.468	-6.659	3.289	-2.621	9.64
a (depth coeff)	42.37	3.72	–	–	43.14	36.23	–
b (flow rate coeff)	-7.109	–	- 0.01354	–	-4.405	–	0.004231
c (temp coeff)	12.16	–	–	0.09177	–	-16.06	-0.1703
DIC	0.02266	0.2804	12.74	12.36	0.02729	0.03374	14.23

According to Table 10, best fit model should be the first one (smallest DIC, of 0.02266) which has all the three parameters namely, depth, flow and temperature driving the model to failure. Currently, work is being done on this section to determine the Bayesian p-value.

### **5.2.2 DIC Model Analysis for NASA Data**

The example script in Table 3 was run for temperature and pressure DIC values. The results of this is shown in Table 11.

**Table 11. DIC and p-values for the NASA Example Data**

<i><b>Parameters</b></i>	<i><b>Equation 5( P and T)</b></i>	<i><b>Equation 6 (T)</b></i>	<i><b>Equation 7 (P)</b></i>
DIC	36.67	35.41	38.68
Bayesian p-value	0.19	0.21	0.26

According to model selection via DIC, among the three models equation 6 (temperature model) has the smallest DIC. But, as seen in Table 11 there is just a slight variation in the p-values for the three model and the p-values are not far from 0.5, so equation 5 (both temperature and pressure model) is selected. Both the variables are kept for possible future flexibility. When DIC and p-values are similar, it is recommended that the model with the most parameters be selected.

The next section outlines about second part of this thesis, the design for CFEL safety circuit.

## 6.0 CFEL Key Features

The testing bay will be the heart of CFEL where the flooding experiments will be carried out, see Figure 14. During experiments, water will be rapidly introduced into the testing bay. Prior executing experiments, researchers will need to enter the testing bay to configure various experiments. To avoid personnel injury, it is imperative that the CFEL water flow systems are not activated while researchers are present in the testing bay.

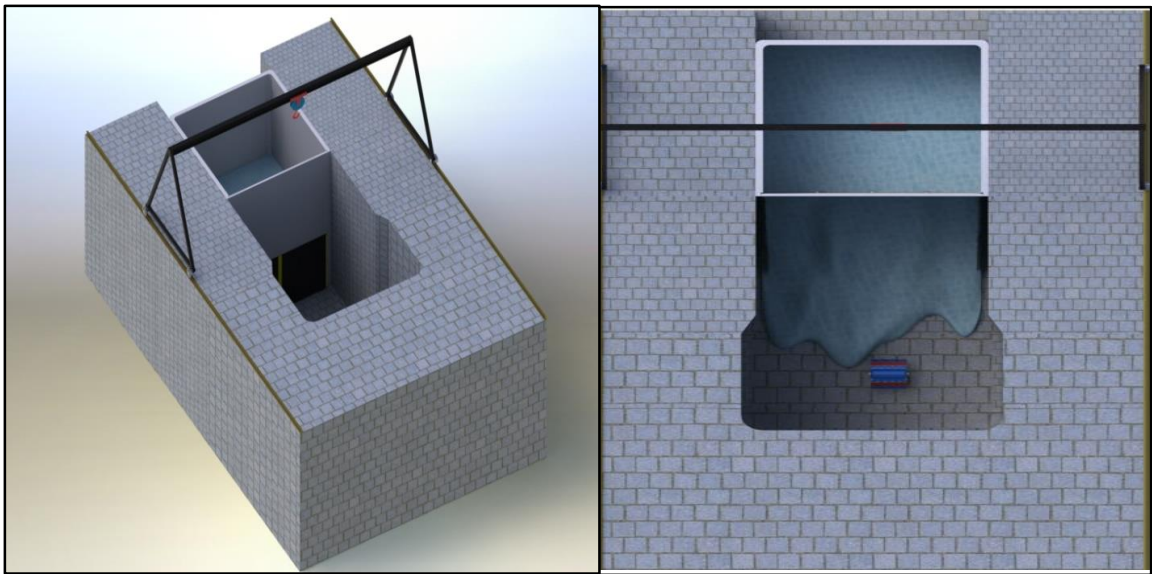


**Figure 14. Testing bay.**

To address the personnel safety issue, a safety strategy was devised that takes advantage of the overall CFEL design. Key features of the CFEL design are depicted in Figure 15. For water to flow, the system pump must be activated and the flow control valve must be open. Additionally, personnel must be in the testing bay to be subject to the hazard. Thus, a safety strategy coupling pump and valve status and personnel access was developed.

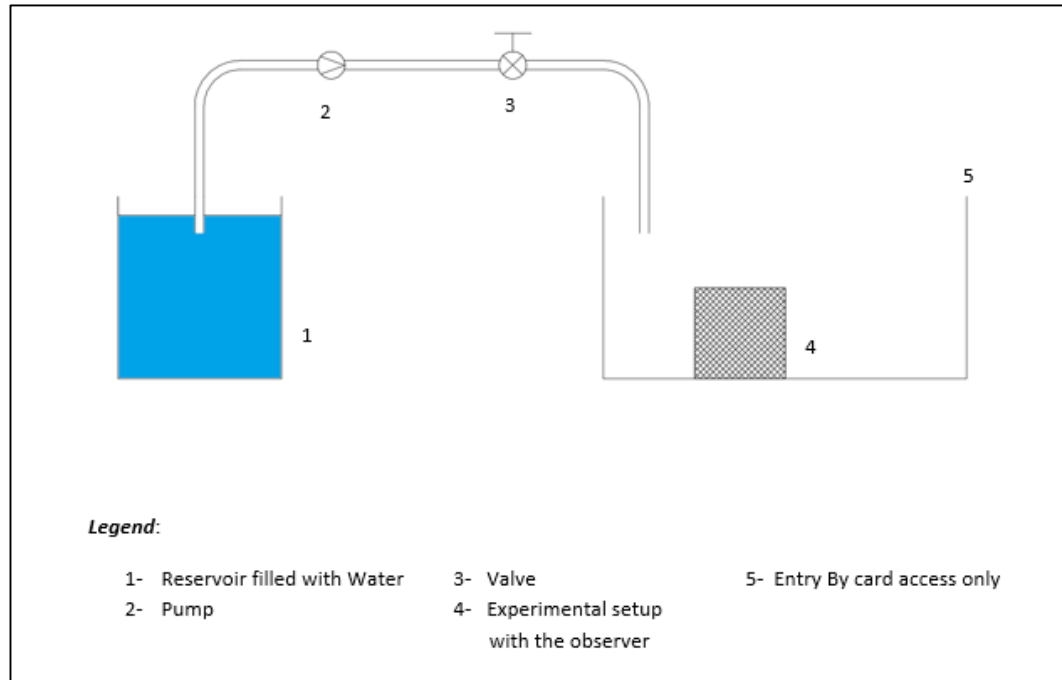


**Figure 15. The key features of CFEL.**

## 6.1 Safety Circuit Design

The CFEL safety circuit ensures no water flow occurs during configuration of the experiment within the testing bay. That is, the safety circuit provides personnel protection while they are located in the below grade testing bay by preventing water flow. The safety circuit was particularly designed to provide the safety requirement in CFEL by protecting the person when they are at the testing bay when the experimental set up is being done. It ensures that the flow control like the pumps and the vales are not activated at that time and only switched on when the experiments begin with no personnel in the testing bay.

Two prototypes of the safety circuit have been designed. One circuit is a combination of AND gates and NOT gates. The other way is by the use of a 2:1 MUX

(multiplexer) with two data inputs and a select line. Both of them use the Boolean expression from the Truth Table (T-T) which is simplified using the Karnaugh map (K-map).

The safety circuit design begins with construction of a four -Variable T-T. Inputs to the T-T are Experimenter (A), Card (B), Pump (C) and Valve (D) (Figure 15). The reason for choosing the above parameters is as follows: - Once the Experimenter has the access to the testing bay, he must then configure the required experimental setup. Once he leaves the bay, the next step would be the activation of water flow with the help of Pump and Valve. So, these four parameters form the premise as the four variable of the T-T (Table 12).

**Table 12. Truth Table**

<b>Cell No</b>	<b>Experimenter- A</b>	<b>Card- B</b>	<b>Pump- C</b>	<b>Valve- D</b>	<b>Output- Y</b>
0	0	0	0	0	0
1	0	0	0	1	0
2	0	0	1	0	0
3	0	0	1	1	0
4	0	1	0	0	0
5	0	1	0	1	0
6	0	1	1	0	0
7	0	1	1	1	0
8	1	0	0	0	0
9	1	0	0	1	0
10	1	0	1	0	0
11	1	0	1	1	0
12	1	1	0	0	1
13	1	1	0	1	0
14	1	1	1	0	0
15	1	1	1	1	0

The T-T is constructed as follows: For an n-Variable T-T, the number of input combinations required are  $2^n$ , so in this case we have four variables and  $2^4 = 16$  input combinations. These combinations are then written in BCD (Binary Coded Decimal) or the 8-4-2-1 format from 0(0000) to 15(1111). For example, Cell No 12 of the T-T (Table 12), where Experimenter and the Card is high (1) meaning the former has access to the bay and the Pump and the Valve are low (0) i.e. they are closed at the start of the experiments. Once the truth table is obtained we need to a boolean expression of the above mentioned condition. K-maps are used to facilitate the simplification of Boolean algebra functions. The Boolean function described by the following truth table. Since we have four input variables, they can be combined in 16 different ways, so the truth table has 16 rows, and the Karnaugh map has 16 positions. The Karnaugh map is therefore arranged in a  $4 \times 4$  grid [10].

The values from the T-T are transferred onto two-dimensional grid with the cells arranged in gray code. Gray code is way of encoding numbers such that the adjacent numbers just change by one bit. The cell positions are the representation of the input combinations and the cell values is its analogous output value from the T-T. Groups of 1's and 0's are identified and grouped together as single group or a pair or quadruplets. This represents the canonical form of the logic in the original T-T. For example, 1's are in Cell No. 12 and hence grouped as a single term. The canonical form for this cell is  $AB\bar{C}\bar{D}$ . Thus, a Boolean expression is obtained for the logic is given in equation (23). The K-map for the T-T is shown in Figure 16.

		CD			
		$\bar{C}\bar{D}$	$\bar{C}D$	$CD$	$C\bar{D}$
AB	$\bar{A}\bar{B}$	0	1	3	2
	$\bar{A}B$	0	0	0	0
AB	$\bar{A}B$	4	5	7	6
	$\bar{A}B$	0	0	0	0
AB	$\bar{A}B$	12	13	15	14
	$\bar{A}B$	0	0	0	0
AB	$\bar{A}B$	8	9	11	10
	$\bar{A}B$	0	0	0	0

Figure 16. K-map.

$$Y = A \bullet B \bullet \bar{C} \bullet \bar{D} \quad (23)$$

Once the boolean expression is obtained the next step is to construct a logic diagram for the expression obtained in equation 22. This is as shown in Figure 17.

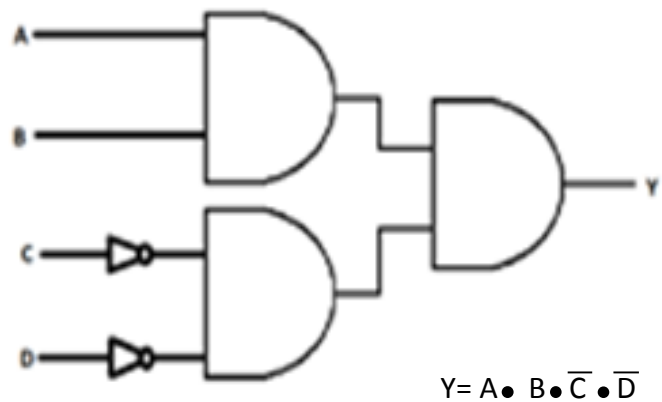
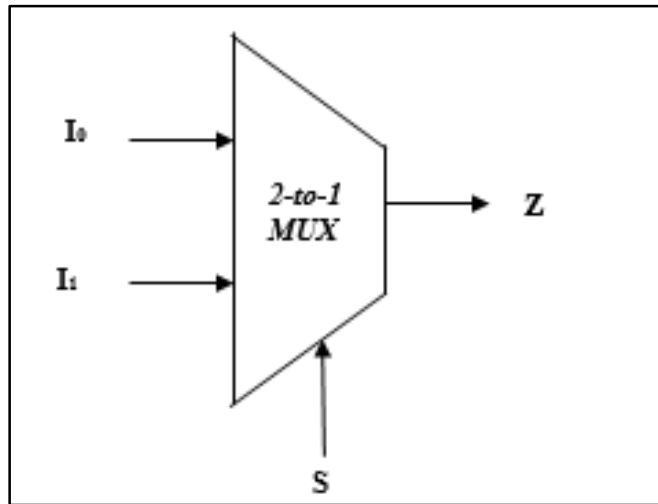


Figure 17. First safety circuit logic.

The second safety circuit uses a MUX (Figure 18). The input of the two data lines are zero and an AND combination of Experimenter and the Card given by  $I_0$ . The select line is the OR combination of the Pump and the Valve given by  $S$ . The output is low (output is 0) only if the Experimenter and Card entry is high (if the experimenter has an access) and the Pump and Valve entry is low (before the start of the flooding experiments when the Pump and the Valve is closed).



**Figure 18. Second Safety Circuit using a 2:1 MUX.**

Using the information, the equation for 2:1 MUX is shown below in equation (24) and the output is shown in equation (25).

$$Z = I_0 \bullet S + I_1 \bullet \bar{S} \quad (24)$$

Where  $I_0 = A \bullet B$  and  $I_1 = 0$  and  $S = C + D$ ,

$$\bar{S} = \overline{C + D} = \bar{C} \bullet \bar{D}$$

$$\text{So, } Z = A \bullet B \bullet \bar{C} \bullet \bar{D} \quad (25)$$



### 6.1.1 Safety Circuit Implementation

Both safety circuit designs were implemented on a breadboard and verified by connecting an LED to the output from each of the safety circuits. The first part in circuit implementation is selection of the logic gates from available digital logic families and the second part is choosing the company that manufactures the logic family. Some common logic families are Resistor-Transistor Logic (RTL), Transistor- Transistor Logic ( TTL), Diode– Transistor logic (DTL) and Complementary Metal-Oxide-Semiconductor logic (CMOS) For the two safety circuits designed in equations 23 and 25, Low power Schottky (LS) logic is selected from TTL . The TTL logic family in general has many advantages when compared to the other logic families. High noise immunity, wide operating temperatures, easy interface with high-level circuits are among the many and the key features of LS are low power consumption and short propagations delays [10].

For the second part, Texas instruments (TI) was chosen as the primary manufacturer. There was no specific reason for choosing TI, other than the history attributed to the TTL family in TI. The TTL family of integrated circuits was introduced about 20 years ago by TI. All the manufacturer of TTL chips use a common naming system as “SN74LS01”. The Prefix SN indicates that this chip was manufactured by TI. The other company have their prefix codes. The numeric code 74 indicates that the chip complies to the requirements of the civilian computer industry, being able to operate over a temperature range of 0° to 70° C. The letters LS indicate which subfamily the chip belongs

to. Finally, the last two digits indicate the logical function performed by the chip such as AND, OR , NOT or inverter logic etc. [11].

The logic components ordered from the TI were AND gate (SN74LS08), OR gate(SN74LS32) NOT gate (SN74LS04) and 2:1 MUX (SN74LS157). The circuit diagram, truth table of these gates are in Appendix D. Before the construction of the circuit an online simulation, tool was used to verify the logic for both safety circuits. The first safety circuit is shown in Figure 19. The inputs to the gates is a digitally simulated voltage either 0 or 1 and cell no 12 of T-T in table 11 is verified for the first safety circuit.

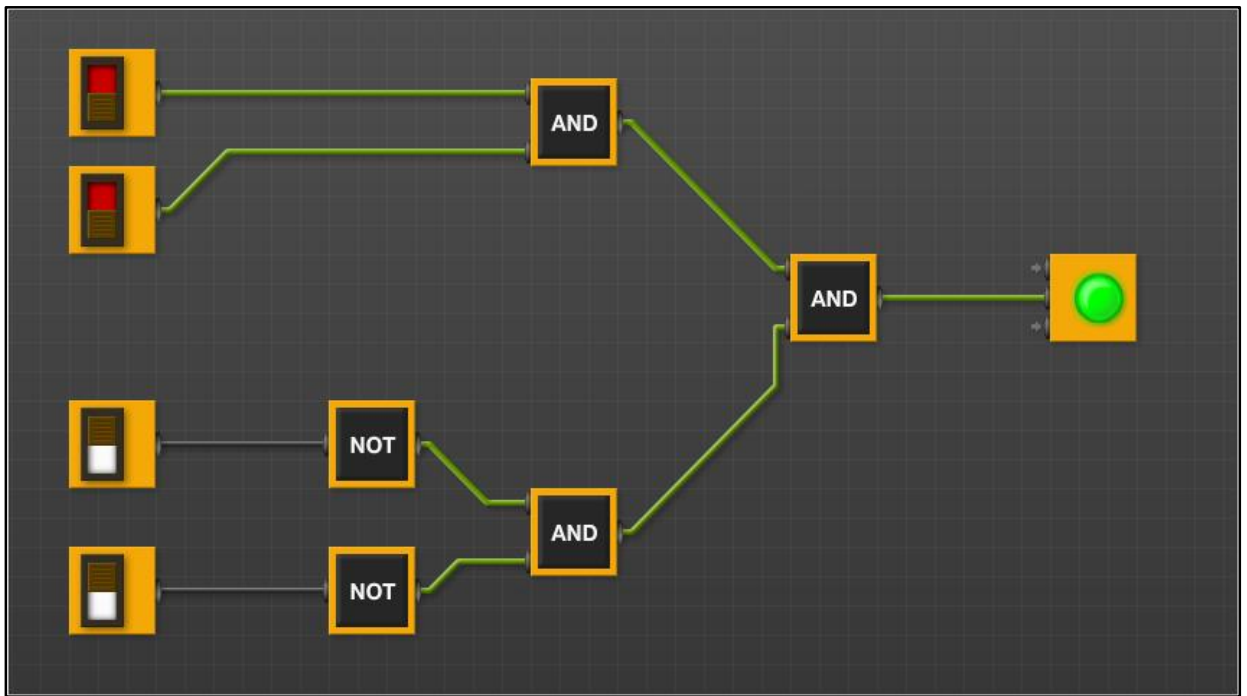


**Figure 19. Online simulation of first safety circuit.**

The second safety circuit using the MUX is broken down to the internal circuit with logic gates for an easier understanding. The dotted lines in Figure 20 shows the MUX's

internal circuits consisting of AND, OR and an inverter. Figure 21 shows the online simulation of the second safety circuit.

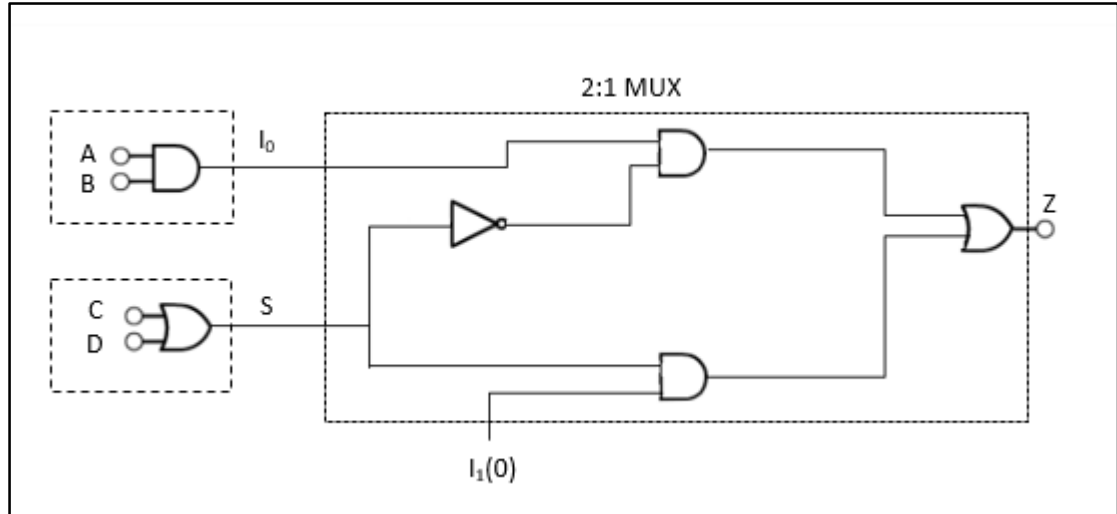


**Figure 20. Second safety circuit with 2:1 MUX's internal circuit.**

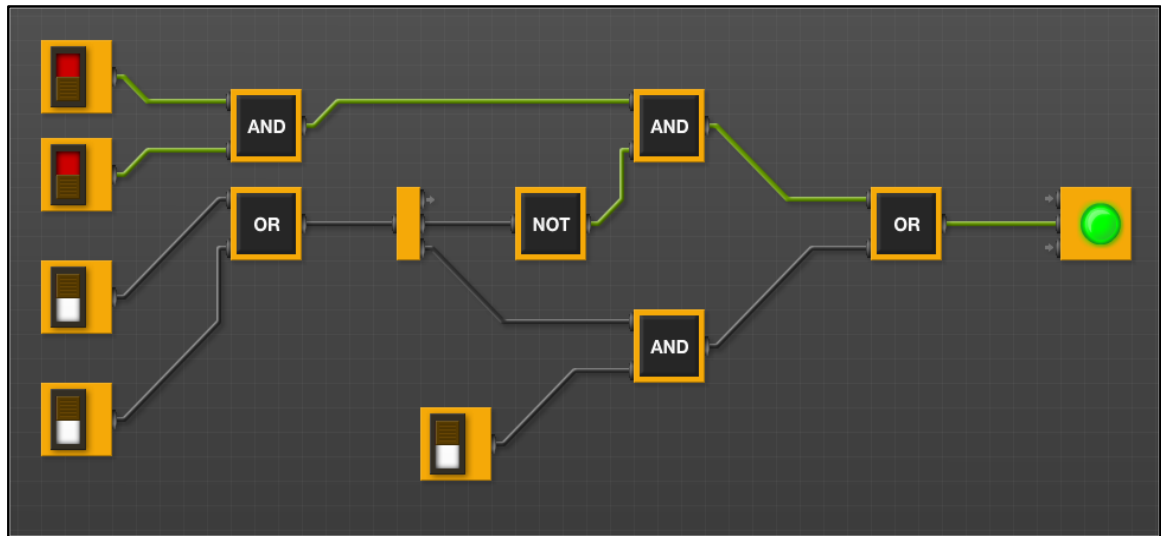


**Figure 21. Online simulation of second safety circuit.**

The online simulation was followed by building both the safety circuits on the bread board. Figure 22 shows the first safety circuit on bread board. The circuit is read from

right to left as, the first gate is the NOT followed by two AND gates. The output of the last AND gate is connected to a 200 ohms ( $\Omega$ ) resistor to protect the Light Emitting Diode (LED) from trying to draw too much current. The inputs to the gates is 5V from a DC power supply and ground (0V) is connected at the required terminals. The combination of cell no 12 from the T-T (Table 12) is verified and output for this combination is high (1) and so the LED glows.

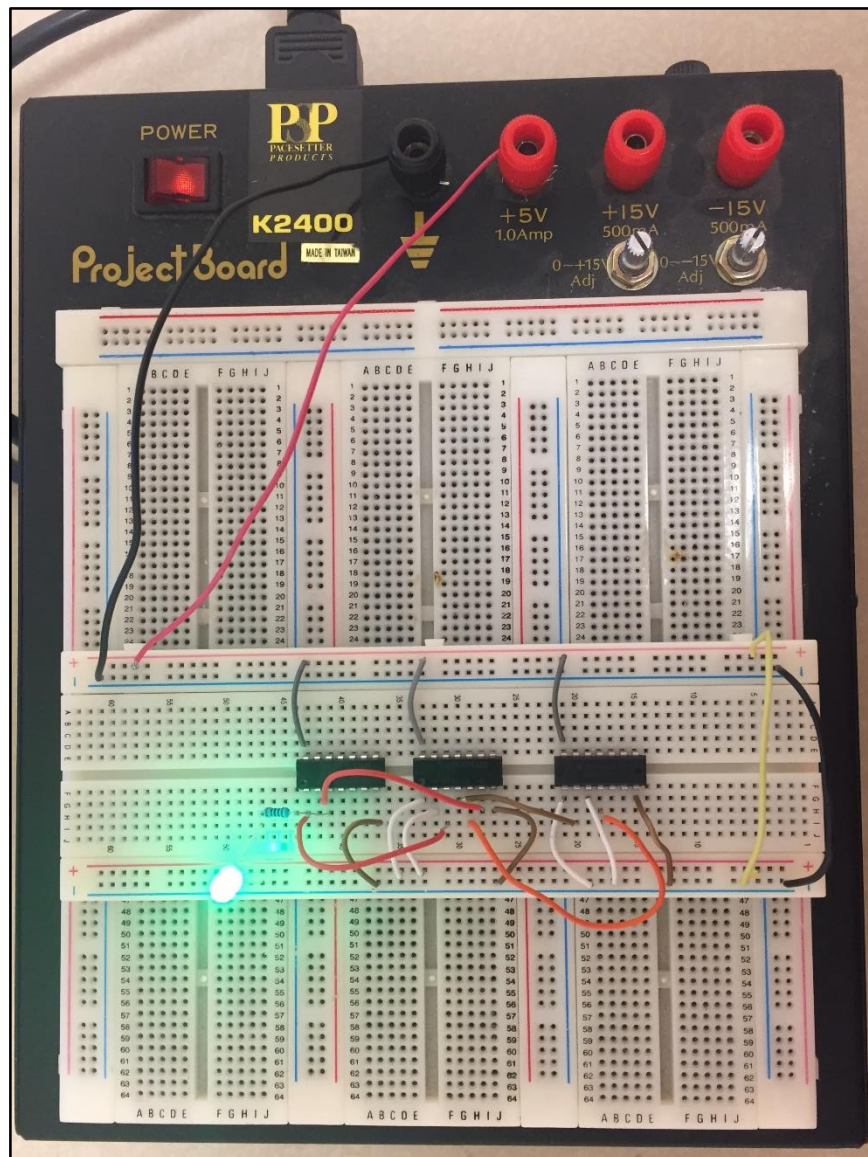


Figure 22. Implementation of first safety circuit on breadboard.

The second safety circuit is implemented in a similar way as shown in Figure 23. The circuit is read from left to right with OR gate combinational logic followed by AND gate for the select input of the MUX. The output of MUX is connected to a 200  $\Omega$  resistor and then to a LED. The output is high (1) as the same cell no 12 of T-T is verified.

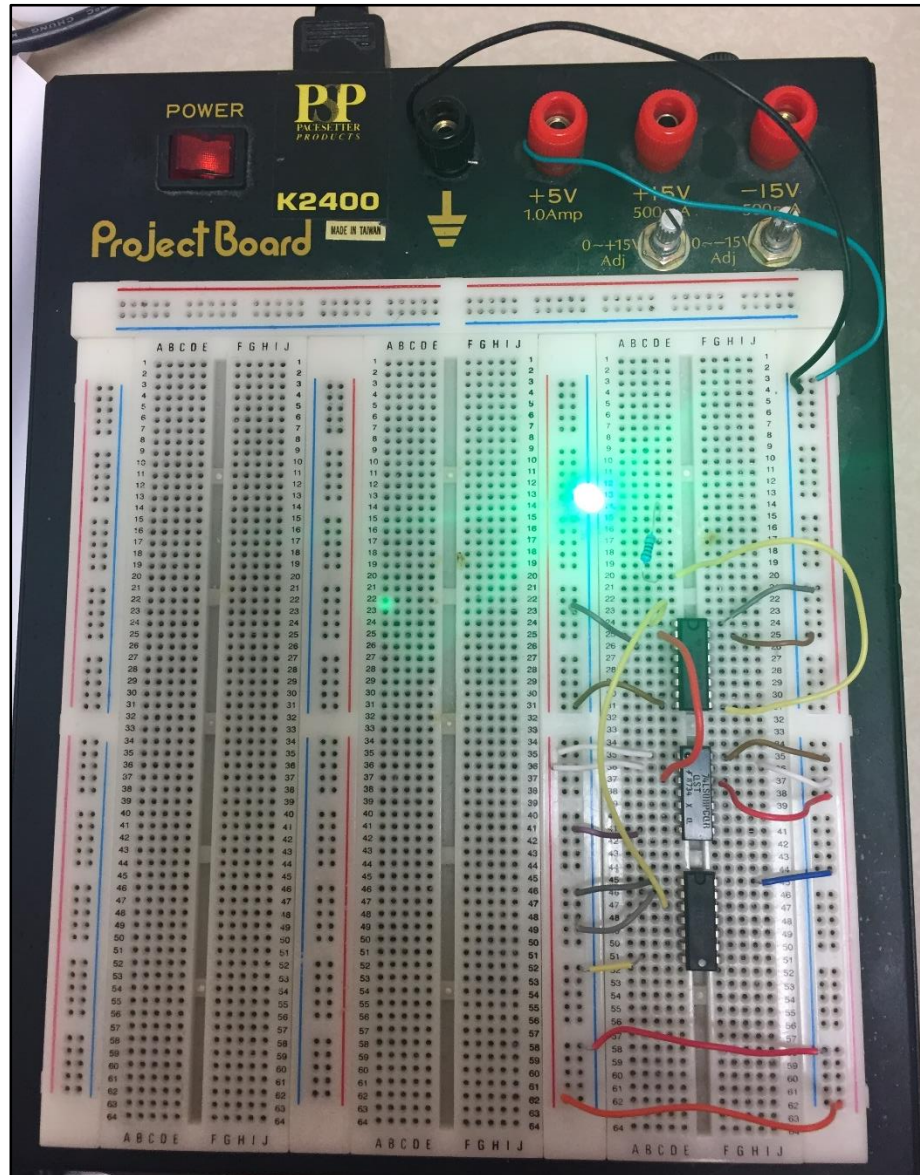


Figure 23. Implementation of second safety circuit on breadboard.

## 6.2 Reliability of Components

Any component or system operating changes its state as the time evolves and at any given point of time they are either running successfully or have failed. Any working component will fail in its period of time. A component is generally classified as repairable or non-repairable and is assumed to have two states namely, failed state and working state. If a component is repairable and has failed, it will continue to remain in that state of time until it is repaired. Once the repair is completed it transcends back to functioning state. It is assumed that this component is back to its original state and its “almost in new condition” The change from a functioning to a failed state is failure while the change from a failure to a functioning state is referred to as repair. This cycle of failure to repair will continue for a repairable component.

The reliability,  $R(t)$ , of a component or system is defined as the probability that the component or system remains operating from time zero to time  $t_1$ , given that it was operating at time zero. Reliability is commonly quantified in terms of one of the category of failure rate ( $\lambda$ ) known as the Mean Time to failure (MTBF). The aim of this thesis to check for the reliability of the two safety circuits given the MTBF. The following sections provide more information on MTBF,  $\lambda(t)$  and how they all are related to each other.

### 6.2.1 Reliability Prediction Definitions

*Failure rate  $\lambda(t)$* : Rate at which components fail per unit time. General notation for failure rate is ‘X failures per million hours’ but the common unit used in semiconductor



industry is FIT (Failures In Time). FIT gives the number of failures in one billion hours of operation. Hence,  $FIT = 10^9 / MTBF$ .

*Mean time between failure(MTBF)*: is a basic measure of reliability for repairable items. It is defined as the arithmetic mean value of session time between two failures where the system is functional. The following illustration (Figure 24) explains MTBF graphically:

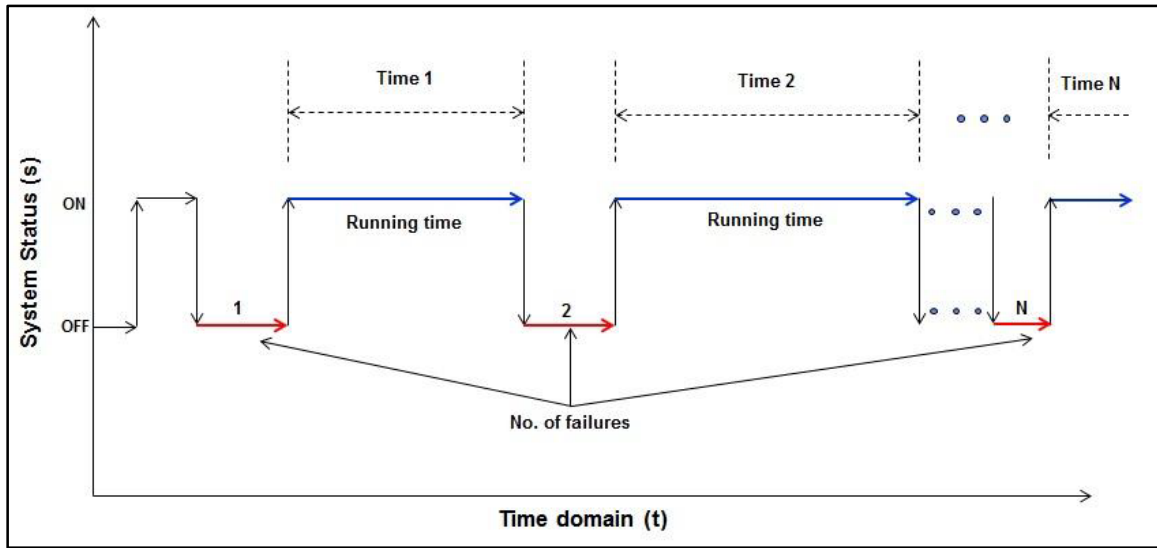


**Figure 24. Understanding MTBF.**

The time when the system is functional is mentioned as “Running time” and denoted as “Time 1, Time 2 . . . Time N”, while the number of failures is denoted as “1, 2 . . . N”. Hence, MTBF can be expressed as:

$$MTBF = [Time\ 1 + Time\ 2 + \dots + Time\ N] / [N]$$

MTBF is usually expressed in terms of hours. MTBF can also be calculated as the inverse of the failure rate,  $\lambda$ , for constant failure rate.

$$MTBF = \frac{1}{\lambda} \quad (26)$$

The following equation (25) gives the relationship between  $R(t)$ , MTBF and  $\lambda(t)$

$$MTBF = \frac{1}{\lambda} \quad (27)$$

Where,

$R(t)$ : Reliability of the component

MTBF: Mean Time Between Failure

$t$ : hours of operations

$\lambda$  : failure rate

The next section provides an insight about components life span i.e. most components lifetimes can be represented using a simple curve called the bathtub curve [12].

### 6.2.2 Bathtub Curve

A bathtub curve as the name suggests has a plot like the shape of a “bathtub” and is a graph of time vs failure rates. This curve has been widely accepted by the reliability community over the years. The life of a population of units can be divided into three distinct periods. Figure 25 shows the general plot of bathtub curve for devices. As seen, the first period or initial stages at time zero, is characterized by a high but a decreasing failure rate. This occurrence is mainly seen in the populations units that are weaker when compared to the others. This region is known as the Early Failure period (also referred to as infant mortality period and is expected to last for a few months. The next region on the graph is the flat portion where the failure rates are low and constant. This region is referred to as the intrinsic failure period (also called the stable failure period or the useful period). Most components spend their lifetime in this region of the bathtub curve. The last region is the wear-out failure period where the components that survives the two



regions now may begin to fail due to aging or degradation. The failure rate is rapidly increasing with time [12] & [13].

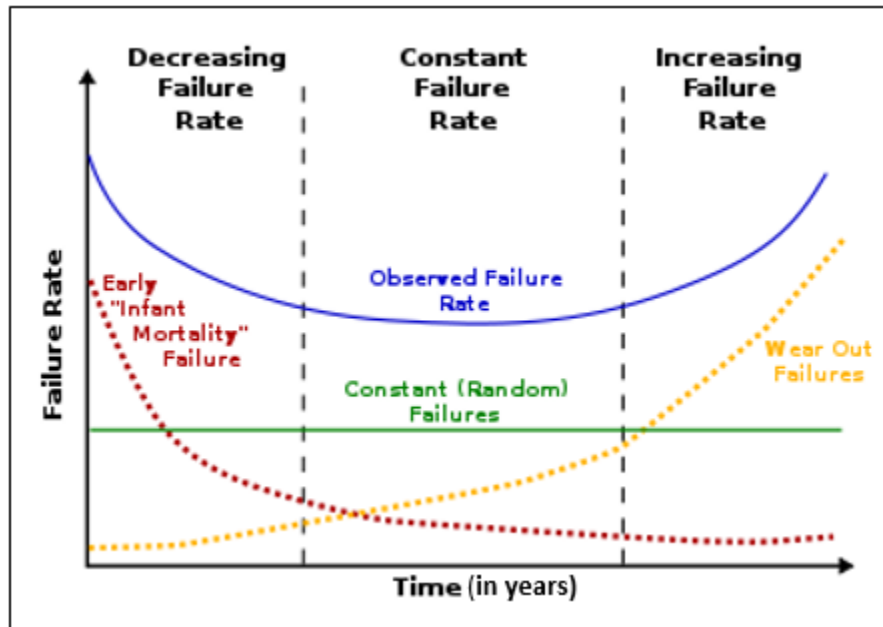


Figure 25. Typical bathtub curve.

The TI website lists the MTBF rates for components chosen for the two safety circuits [14]. Appendix E lists the MTBF and the bathtub curve for the components used. The last section of safety circuit analysis deals with calculation of  $R(t)$  given the value of  $t$  and fault tree representations. Finally, the more reliable safety circuit between the two can be determined.

### 6.2.3 $R(t)$ Calculations

Using the information from the TI website (

Appendix E) for the components used in building of the two safety circuits and using equation (27) for  $R(t)$ , we have

$$t = 1000 \text{ hours, MTBF} = 1.38 \times 10^9 \quad (28)$$

$$R(t) = e^{-\lambda t} = e^{-(t/\text{MTBF})}$$

$$R(t) = e^{-(1000/1.38 \times 10^9)} \quad [\text{using 28}]$$

$$R(t) = 0.9999992754 \quad (29)$$

Since all the logic components have the same MTBF,  $R(t)$  also remains the same. Next, is the calculation of complete system  $R(t)$  i.e.  $R_{\text{sys}}(t)$  for safety circuit 1 and safety circuit 2.

Before  $R_{\text{sys}}(t)$  is calculated for the two safety circuits, it is necessary to see the available methods to compute the system reliability from component reliabilities. the two commonly used methods are Reliability Block Diagrams (RBD) and Fault Trees (FT). The two will be discussed in detail in the coming sections.

#### 6.2.4 Reliability Block Diagrams

A Reliability Block Diagram(RBD) is a diagrammatic approach that shows individual component reliability contributes to the entire system's reliability ( $R_{\text{sys}}(t)$ ) in terms of success or failure. The RBDs are usually represented as blocks either in series or parallel combinations or a combination of both. [15]

For a series circuit as shown in Figure 26, the reliability is calculated as  $R_S = R_A R_B R_C$

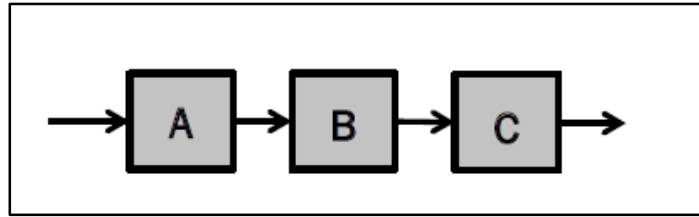


**Figure 26. Components connected in series.**

$$R_s = R_A R_B R_C$$

For a parallel circuit as shown in Figure 27, the reliability is calculated as

$$R_s = (1 - R_A) (1 - R_B) (1 - R_C)$$

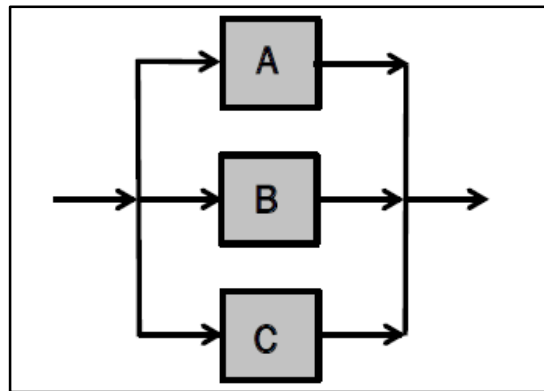


**Figure 27. Components connected in parallel.**

$$R_s = (1 - R_A) (1 - R_B) (1 - R_C)$$

With this information,  $R_{sys}(t)$  for the first safety circuit and second safety circuit can be calculated.

For the first safety circuit, referring to Figure 17, It is observed that all of gates must connected in series for a successful operation, and there are no redundant gates so no parallel circuits. Hence, the RBD equivalent circuit is three blocks connected in as

shown in Figure 28. Block A is the first component; block B is the second component with one inverter gate in series to it. And block C is the third component in the circuit. Each block has  $R(t)$  approximately equal to 0.99 (from equation 28). Also, referring to Figure 26 for series reliability,  $R_{1sys}(t)$ .

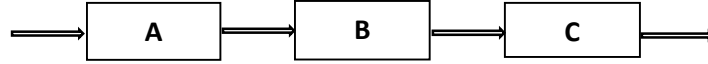


**Figure 28. RBD for the first safety circuit.**

Here,

$$R_A = 0.99$$

$$R_B = 0.99$$

$$R_C = 0.99$$

Therefore,

$$R_{1sys}(t) = 0.99 \times 0.99 \times 0.99 = 0.9703$$

So, first safety circuit is reliable about 97%, under given operation conditions.

For the second safety circuit the reliability of this circuit is a bit complicated as the MUX is made up of internal gates and the individual MTBF of the gates is unknown so, the mux was considered as a single entity or a block and the other two gates as two separate blocks. First component X was the OR gate for the select line **S** and component Y was the AND gate for input **I<sub>0</sub>** and component Z was considered as the MUX.

So, the RBD is similar to the first safety circuit and is shown as in Figure 28.

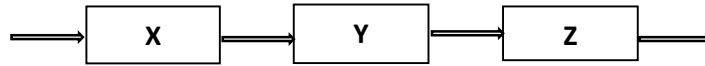


**Figure 29. Second safety circuit RBD.**

Here,

$$R_X = 0.99$$

$$R_Y = 0.99$$

$$R_Z = 0.99$$

Therefore,

$$R_{2sys}(t) = 0.99 \times 0.99 \times 0.99 = 0.9703$$

So, second safety circuit is reliable about 97%, under given operation conditions.

Even though the second safety circuit has the same  $R_{sys}(t)$  as the first safety circuit, the latter is more reliable because of the lesser number of components used and all the rates having the same MTBF rates. The MUX was assumed to be a single entity, but in comparison it's made of several internal logic gates that may have different failure rates impairing the overall MUX's operation in the long run.

### **6.2.5 Fault Tree Analysis**

Fault Tree analysis (FTA) follows a top down approach for failure modeling. Top event is the undesired event and combination of events that lead to it are modelled using gates and events connected with lines. An RBD can easily be converted by replacing the series and parallel paths by OR and AND gates respectively. An OR gate is used when the output event occurs, if at least one of the input events occurs while an AND gate is used

when the output event occurs, if all input events occur. RBD is the modeling of a success event, the Fault Tree (FT) is modeling of a failure event. The two safety circuits are now modelled for unreliability using the FT approach [15].

The FT for the first safety circuit is done by considering the basic or the initial events affecting the seconding events and then the final events. The serious blocks of the RDBs in Figure 26 is replaced by the OR gate. Safety circuit in Figure 17 is modelled using the FT approach shown below in Figure 30.

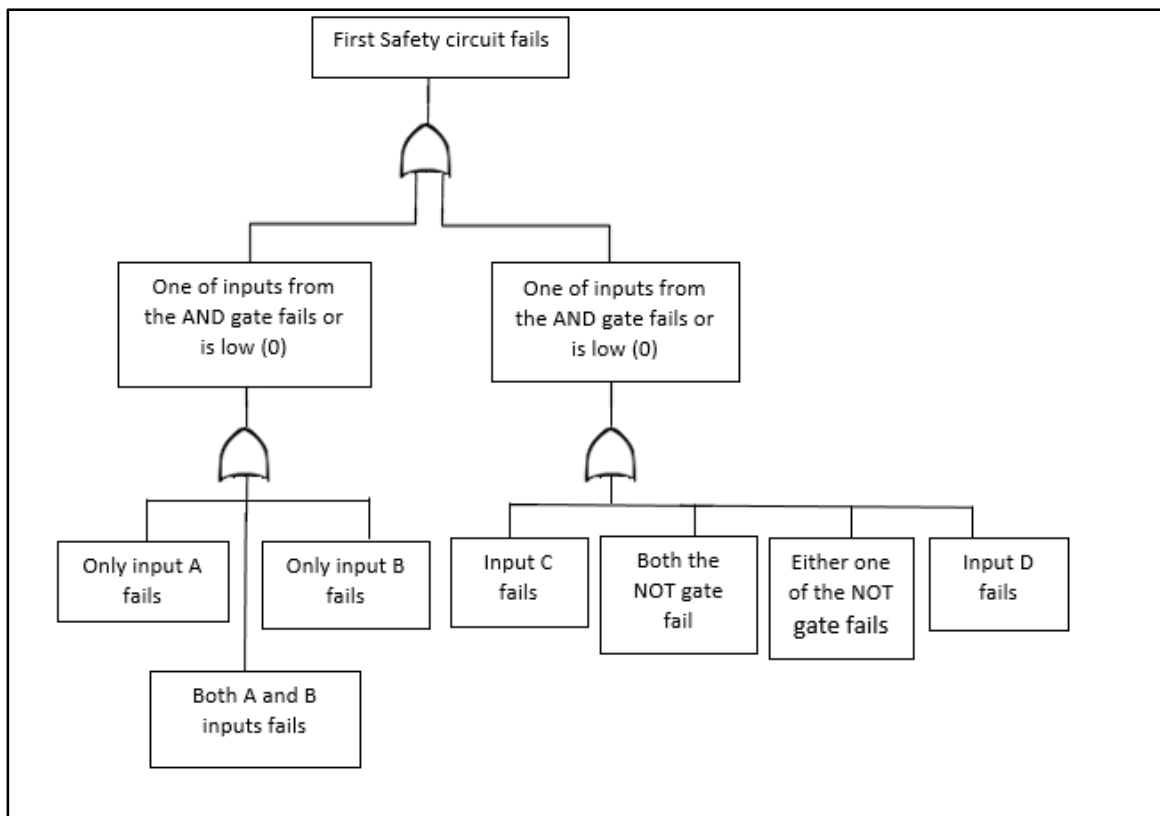


**Figure 30. FT analysis for the first safety circuit.**

The second safety circuit modeling is done similar to the first one, with basic events affecting the secondary and eventually the top event. Referring to Figure 18 for the second safety circuit, the FT analysis is done as shown in Figure 31.

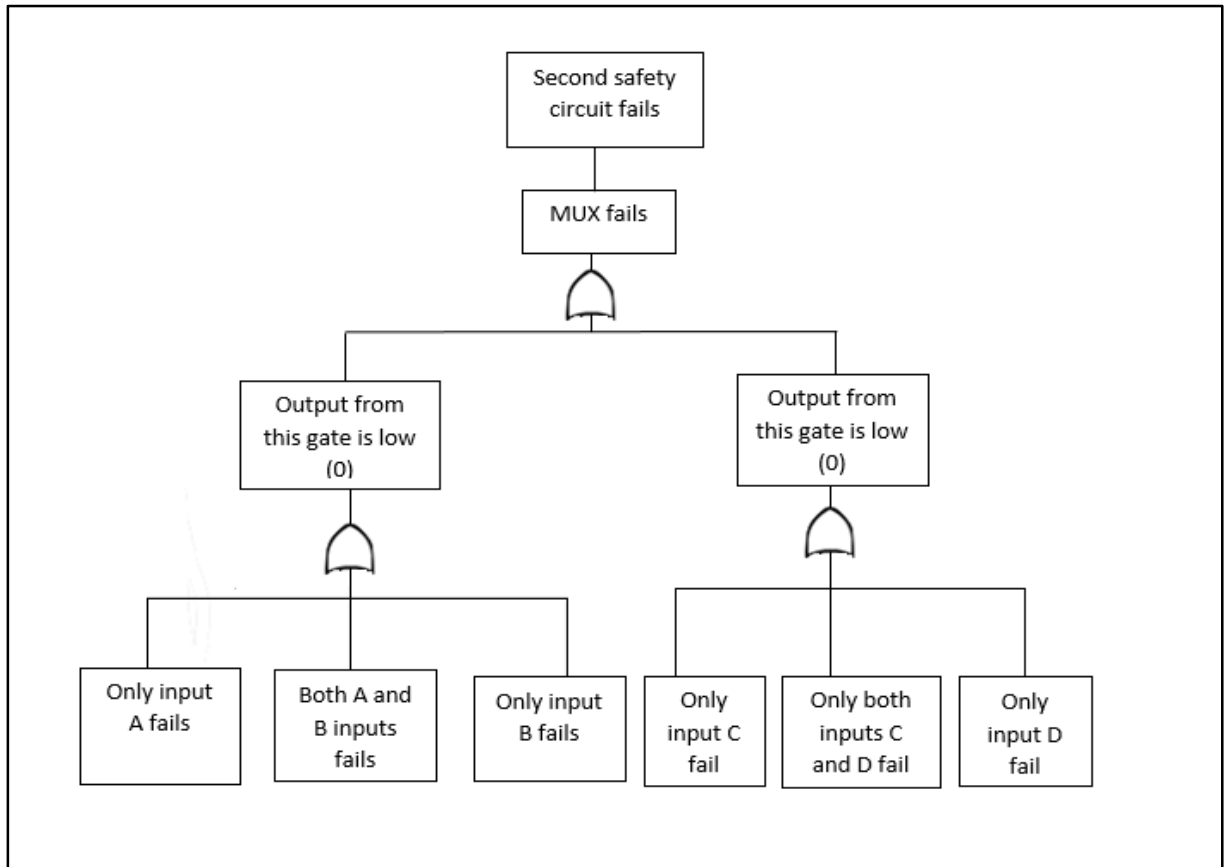


**Figure 31. FT analysis for the second safety circuit.**

Based on the reliability and FTA the first safety circuit is recommended for safe operations at CFEL.

## **7 Conclusion**

Safety is the utmost priority in any industry and with the NPP industry it is the essence of any operational system. This thesis was an attempt to fortify the safety in NPP risk analysis concerning the flooding events. Bayesian models were developed to better understand the risk associated with NPP flooding conditions, and progress is still being made to better quantify the risks. Efforts were also made to develop two safety circuits, the first of its kind for safe operations at CFEL and choosing the better one for efficient operationality. Reliability and FTA was also done to verify for its correctness.

## **8 Future Work**

The path forward for the Bayesian analysis section would be investigate the OpenBUGS link functions in detail and the errors that were found while using certain link functions with different models. A further investigation with small parameter variation would also be considered. The information from the hollow core door modeling would help in future testing of different components and consideration of other variables (if any). Another important future work would be to tie the data and models with the codes currently used by the LWRS effort to model risk safety margin such as Smoothed particle hydrodynamic (SPH). For the safety circuit, it would be to determine if parallel circuits are needed. Investigation on the logic gates of the 74LS series of other companies for comparison on failure rates would also be conducted.

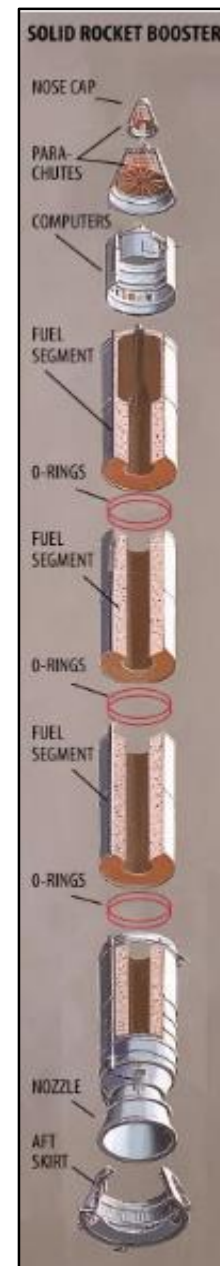
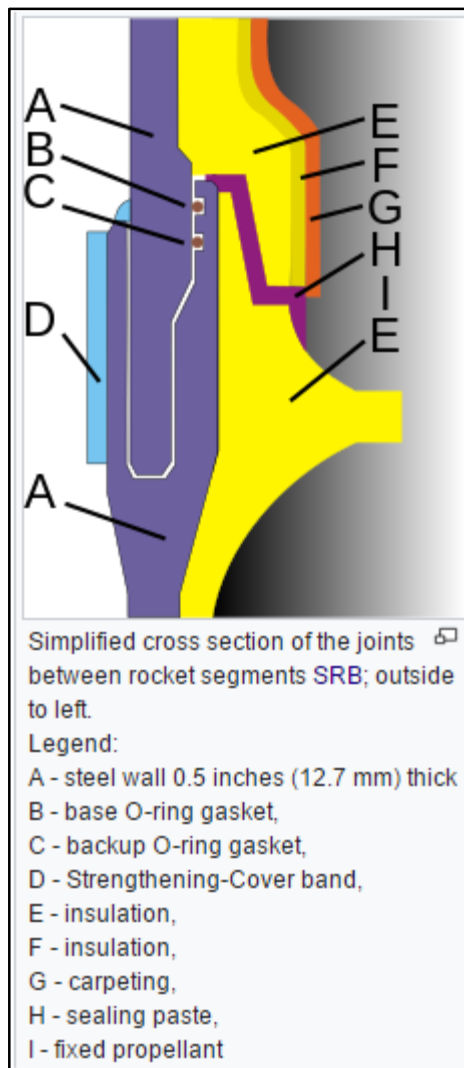


## 9 Bibliography

- [1] I. N. L. Curis Smith, "Light Water Reactor Sustainability Program, Flooding fragility Experiments and Prediction INL/EXT 16-xxxxx".
- [2] D. Kamerman, "The Use of Flooding Fragility Curves in Nuclear Power Plant Risk Analysis, Spring 2016".
- [3] B. Bhandari, "Full Scale Dorr Testing under flooding conditions to Develop Testing Protocol, September 2016".
- [4] D. Kelly and C. Smith, Bayesian Inference for Probabilistic Risk Assessment, Springer, 2011.
- [5] "Chapter IV: The Cause of the Accident," NASA, June 6th, 1986. [Online]. Available: <https://history.nasa.gov/rogersrep/v1ch4.htm#4.12>.
- [6] "Analysis of Discrete Data STAT 504 PSU," [Online]. Available: <https://onlinecourses.science.psu.edu/stat504/node/216>.
- [7] OpenBUGS, "OpenBUGS User Manual," [Online]. Available: <http://www.openbugs.net/Manuals/Contents.html>.
- [8] R. Levy, "Chapter 8 Hierarchical Models," in *Probabilistic Models in the Study of Language*, 2012.
- [9] "Wikipedia," [Online]. Available: [https://en.wikipedia.org/wiki/Deviance\\_information\\_criterion](https://en.wikipedia.org/wiki/Deviance_information_criterion).
- [10] R. S. SAMUEL, Basic Electronics, Sanguine Pearson, 2007.
- [11] [Online]. Available: <http://homepage.divms.uiowa.edu/~jones/logicsim/man/node5.html>.
- [12] Scott Speaks, "vivorpower," [Online]. Available: [http://www.vicorpower.com/documents/quality/Rel\\_MTBF.pdf](http://www.vicorpower.com/documents/quality/Rel_MTBF.pdf).
- [13] "NIST/SEMATECH e-Handbook of Statistical Methods," NIST, 2003. [Online]. Available: <http://www.itl.nist.gov/div898/handbook/apr/section1/apr124.htm>.
- [14] "TI home," Texas Instruments, [Online]. Available: <http://www.ti.com/quality/docs/estimator.tsp>.

[15] A. H. Marvin Rausand, SYSTEM RELIABILITY THEORY Models, Statistical Methods,, Hoboken, New Jersey: A JOHN WILEY & SONS, INC., PUBLICATION, 2004.

## Appendix A



## Appendix B

### 1. Flow model

```
#Flow Rate (F) Model
model {
  for(i in 1:tests) {
    failure[i] ~ dbin(p[i], num.tested)
    # Regression model
    cloglog(p[i]) <- int + b*flow[i]
    # failure.rep[i] ~ dbin(p[i], num.tested) # Replicate values for model validation
    # diff.obs[i] <- pow(failure[i] - num.tested*p[i], 2)/(num.tested*p[i]*(1-p[i]))
    # diff.rep[i] <- pow(failure.rep[i] - num.tested*p[i], 2)/(num.tested*p[i]*(1-p[i]))
  }
  #chisq.obs <- sum(diff.obs[])
  #chisq.rep <- sum(diff.rep[])
  #p.value <- step(chisq.rep - chisq.obs)
  # Prior distributions
  int ~ dnorm(0, 0.0001)
  b ~ dnorm(0, 0.001)
}
data
list(num.tested=1, tests=8, flow = c(291.5,292.5,292.5,297,294.5,292.5,291,294), failure =
c(0,0,1,0,0,1,1,1))
inits
list(int=0, b=0)
```

---

### 2. Temperature model

```
#Temperature (T) Model
model {
  for(i in 1:tests) {
    failure[i] ~ dbin(p[i], num.tested)
    # Regression model
    cloglog(p[i]) <- int + c*temp[i]
    # failure.rep[i] ~ dbin(p[i], num.tested) # Replicate values for model validation
    # diff.obs[i] <- pow(failure[i] - num.tested*p[i], 2)/(num.tested*p[i]*(1-p[i]))
    # diff.rep[i] <- pow(failure.rep[i] - num.tested*p[i], 2)/(num.tested*p[i]*(1-p[i]))
  }
  #chisq.obs <- sum(diff.obs[])
  #chisq.rep <- sum(diff.rep[])
  #p.value <- step(chisq.rep - chisq.obs)
  # Prior distributions
  int ~ dnorm(0, 0.0001)
  c ~ dnorm(0, 0.001)
}
data
list(num.tested=1, tests=8, temp = c(65.98,67.04,66.02,67.67,66.6,66.87,68.33,68.14),
failure = c(0,0,1,0,0,1,1,1))
inits
list(int=0, c=0)
```

---

### 3. Depth and flow model

```
#Flow Rate (F) and Depth (D) Model
model {
  for(i in 1:tests) {
    failure[i] ~ dbin(p[i], num.tested)
    # Regression model
    cloglog(p[i]) <- int + a*depth[i] + b*flow[i]
    #failure.rep[i] ~ dbin(p[i], num.tested)      # Replicate values for model validation
    #diff.obs[i] <- pow(failure[i] - num.tested*p[i], 2)/(num.tested*p[i]*(1-p[i]))
    #diff.rep[i] <- pow(failure.rep[i] - num.tested*p[i], 2)/(num.tested*p[i]*(1-p[i]))
  }
  #chisq.obs <- sum(diff.obs[])
  #chisq.rep <- sum(diff.rep[])
  #p.value <- step(chisq.rep - chisq.obs)
  # Prior distributions
  int ~ dnorm(0, 0.0001)
  a ~ dnorm(0, 0.001)
  b ~ dnorm(0, 0.001)
}
data
list(num.tested=1, tests=8,
     depth = c(23.23,20.75,42.3,21.05,24.22,35.41,40.76,38.85),
     flow = c(291.5,292.5,292.5,297,294.5,292.5,291,294) ,
     failure = c(0,0,1,0,0,1,1,1))
inits
list(int=0, a=0,b=0)
```

---

### 4. Flow and temperature model

```
#Flow Rate (F) and Temperature (T) Model
model {
  for(i in 1:tests) {
    failure[i] ~ dbin(p[i], num.tested)
    # Regression model
    cloglog(p[i]) <- int + b*flow[i] + c*temp[i]
    # failure.rep[i] ~ dbin(p[i], num.tested)      # Replicate values for model validation
    # diff.obs[i] <- pow(failure[i] - num.tested*p[i], 2)/(num.tested*p[i]*(1-p[i]))
    # diff.rep[i] <- pow(failure.rep[i] - num.tested*p[i], 2)/(num.tested*p[i]*(1-p[i]))
  }
  #chisq.obs <- sum(diff.obs[])
  #chisq.rep <- sum(diff.rep[])
  #p.value <- step(chisq.rep - chisq.obs)
  # Prior distributions
  int ~ dnorm(0, 0.0001)
  b ~ dnorm(0, 0.001)
  c ~ dnorm(0, 0.001)
}
data
list(num.tested=1, tests=8, flow = c(291.5,292.5,292.5,297,294.5,292.5,291,294),
     temp = c(65.98,67.04,66.02,67.67,66.6,66.87,68.33,68.14),
     failure = c(0,0,1,0,0,1,1,1))
inits
list(int=0, b=0, c=0)
```

---

## 5. Depth and temperature model

```
#Depth (D) and Temperature (T) Model
model {
  for(i in 1:tests) {
    failure[i] ~ dbin(p[i], num.tested)
    # Regression model
    cloglog(p[i]) <- int + a*depth[i] + c*temp[i]
    # failure.rep[i] ~ dbin(p[i], num.tested) # Replicate values for model validation
    # diff.obs[i] <- pow(failure[i] - num.tested*p[i], 2)/(num.tested*p[i]*(1-p[i]))
    # diff.rep[i] <- pow(failure.rep[i] - num.tested*p[i], 2)/(num.tested*p[i]*(1-p[i]))
  }
  #chisq.obs <- sum(diff.obs[])
  #chisq.rep <- sum(diff.rep[])
  #p.value <- step(chisq.rep - chisq.obs)
  # Prior distributions
  int ~ dnorm(0, 0.0001)
  a ~ dnorm(0, 0.001)
  c ~ dnorm(0, 0.001)
}
data
list(num.tested=1, tests=8, depth = c(23.23,20.75,42.3,21.05,24.22,35.41,40.76,38.85),
temp = c(65.98,67.04,66.02,67.67,66.6,66.87,68.33,68.14),
failure = c(0,0,1,0,0,1,1,1))
inits
list(int=0, a=0,c=0)
```

---

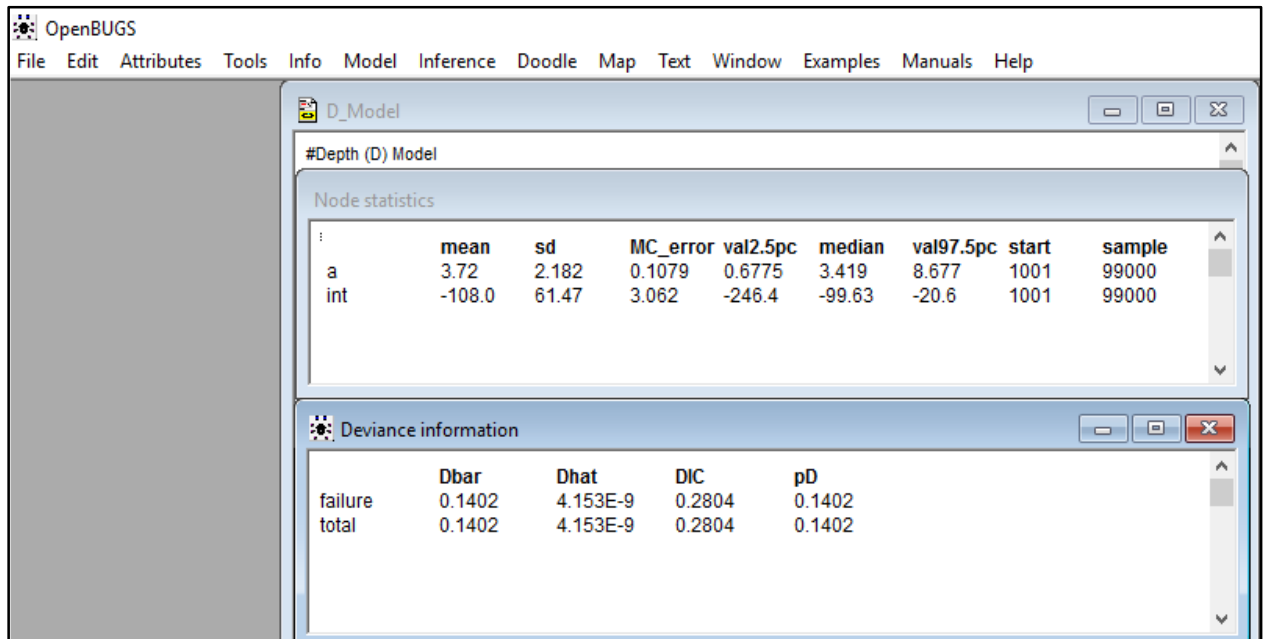
## 6. Depth, flow and temperature model

```
#Flow Rate (F), Depth (D), and Temperature (T) Model
model {
  for(i in 1:tests) {
    failure[i] ~ dbin(p[i], num.tested)
    # Regression model
    logit(p[i]) <- int + a*depth[i] + b*flow[i] + c*temp[i]
    #failure.rep[i] ~ dbin(p[i], num.tested) # Replicate values for model validation
    #diff.obs[i] <- pow(failure[i] - num.tested*p[i], 2)/(num.tested*p[i]*(1-p[i]))
    #diff.rep[i] <- pow(failure.rep[i] - num.tested*p[i], 2)/(num.tested*p[i]*(1-p[i]))
  }
  #chisq.obs <- sum(diff.obs[])
  #chisq.rep <- sum(diff.rep[])
  #p.value <- step(chisq.rep - chisq.obs)
  # Prior distributions
  int ~ dnorm(0, 0.0001)
  a ~ dnorm(0, 0.001)
  b ~ dnorm(0, 0.001)
  c ~ dnorm(0, 0.001)
}
data
list(num.tested=1, tests=8, depth = c(23.23,20.75,42.3,21.05,24.22,35.41,40.76,38.85),
flow = c(291.5,292.5,292.5,297,294.5,292.5,291,294) ,
temp = c(65.98,67.04,66.02,67.67,66.6,66.87,68.33,68.14),
failure = c(0,0,1,0,0,1,1,1))
inits
list(int=0, a=0, b=0, c=0)
```

---

# Appendix C

## 1. Depth Model



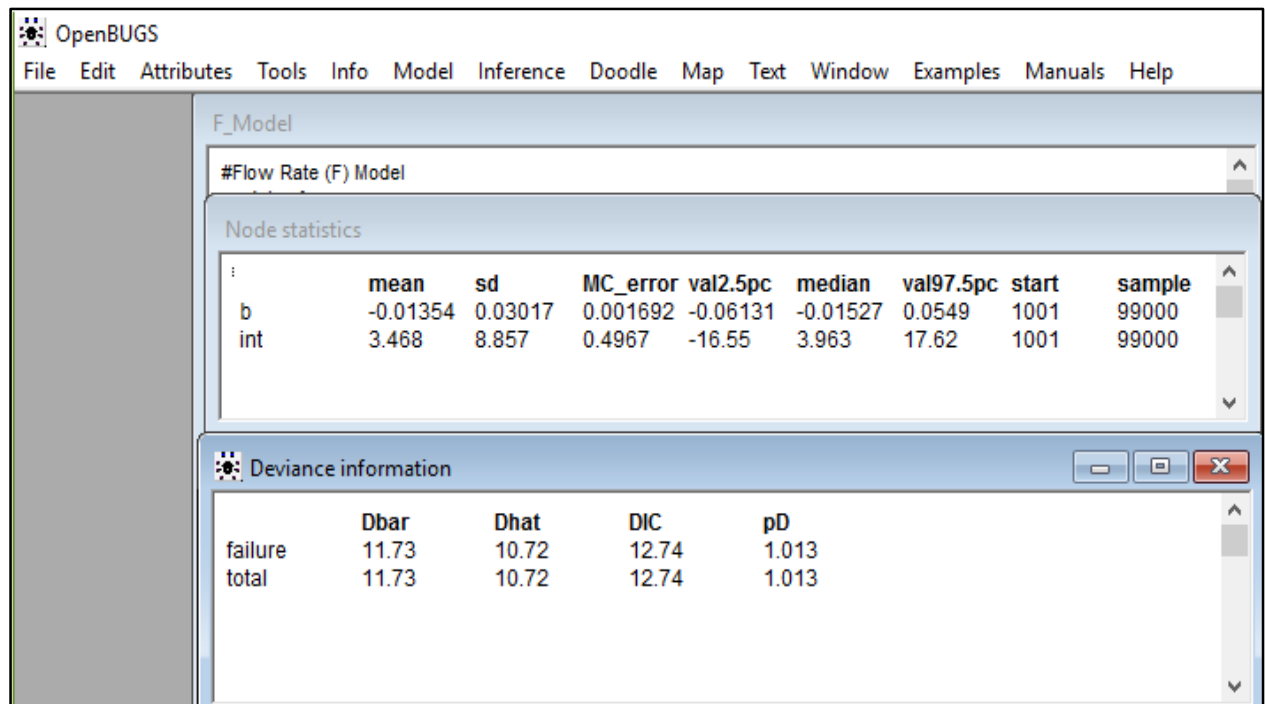
The screenshot shows the OpenBUGS software interface. The main window displays the results for the '#Depth (D) Model'. It includes a menu bar at the top with options like File, Edit, Attributes, Tools, Info, Model, Inference, Doodle, Map, Text, Window, Examples, Manuals, and Help. Below the menu, there are two main panels. The top panel, titled 'Node statistics', shows a table of results for parameters 'a' and 'int'. The bottom panel, titled 'Deviance information', shows a table of results for 'failure' and 'total'.

	mean	sd	MC_error	val2.5pc	median	val97.5pc	start	sample
a	3.72	2.182	0.1079	0.6775	3.419	8.677	1001	99000
int	-108.0	61.47	3.062	-246.4	-99.63	-20.6	1001	99000

	Dbar	Dhat	DIC	pD
failure	0.1402	4.153E-9	0.2804	0.1402
total	0.1402	4.153E-9	0.2804	0.1402

## 2. Flow Model



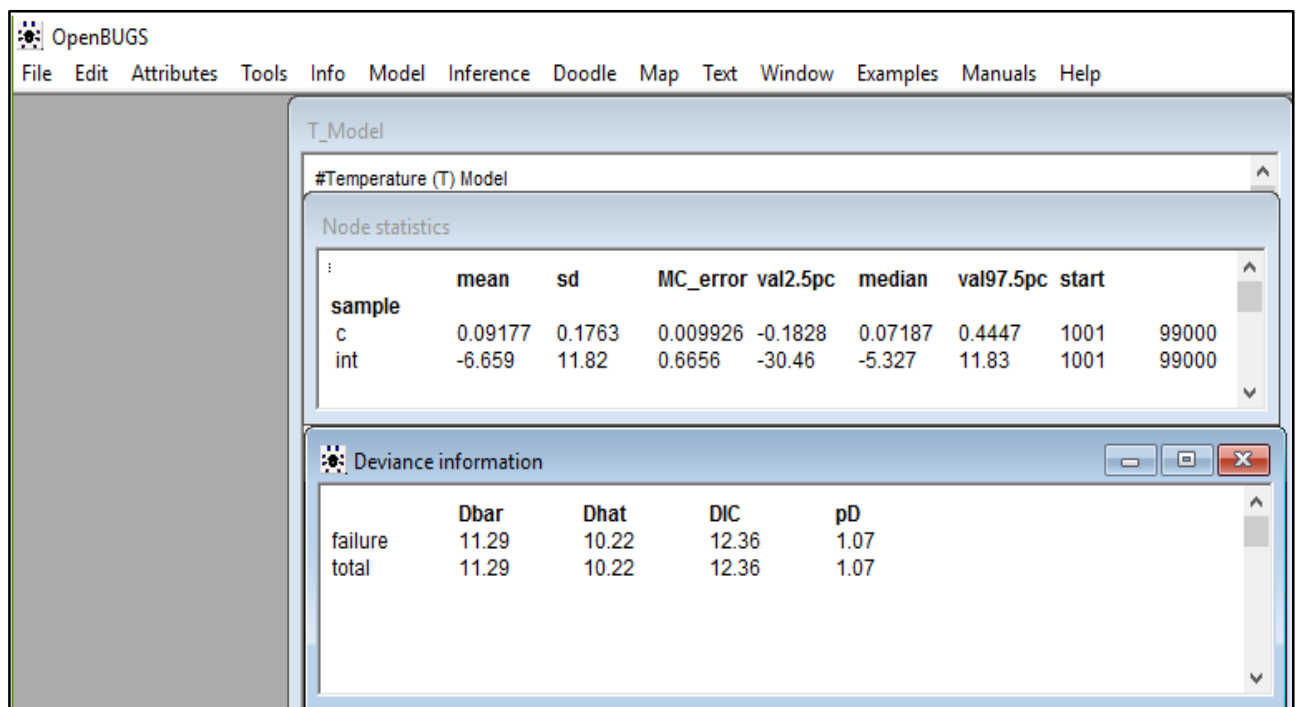
The screenshot shows the OpenBUGS software interface. The main window displays the results for the '#Flow Rate (F) Model'. It includes a menu bar at the top with options like File, Edit, Attributes, Tools, Info, Model, Inference, Doodle, Map, Text, Window, Examples, Manuals, and Help. Below the menu, there are two main panels. The top panel, titled 'Node statistics', shows a table of results for parameters 'b' and 'int'. The bottom panel, titled 'Deviance information', shows a table of results for 'failure' and 'total'.

	mean	sd	MC_error	val2.5pc	median	val97.5pc	start	sample
b	-0.01354	0.03017	0.001692	-0.06131	-0.01527	0.0549	1001	99000
int	3.468	8.857	0.4967	-16.55	3.963	17.62	1001	99000

	Dbar	Dhat	DIC	pD
failure	11.73	10.72	12.74	1.013
total	11.73	10.72	12.74	1.013

### 3. Temperature Model



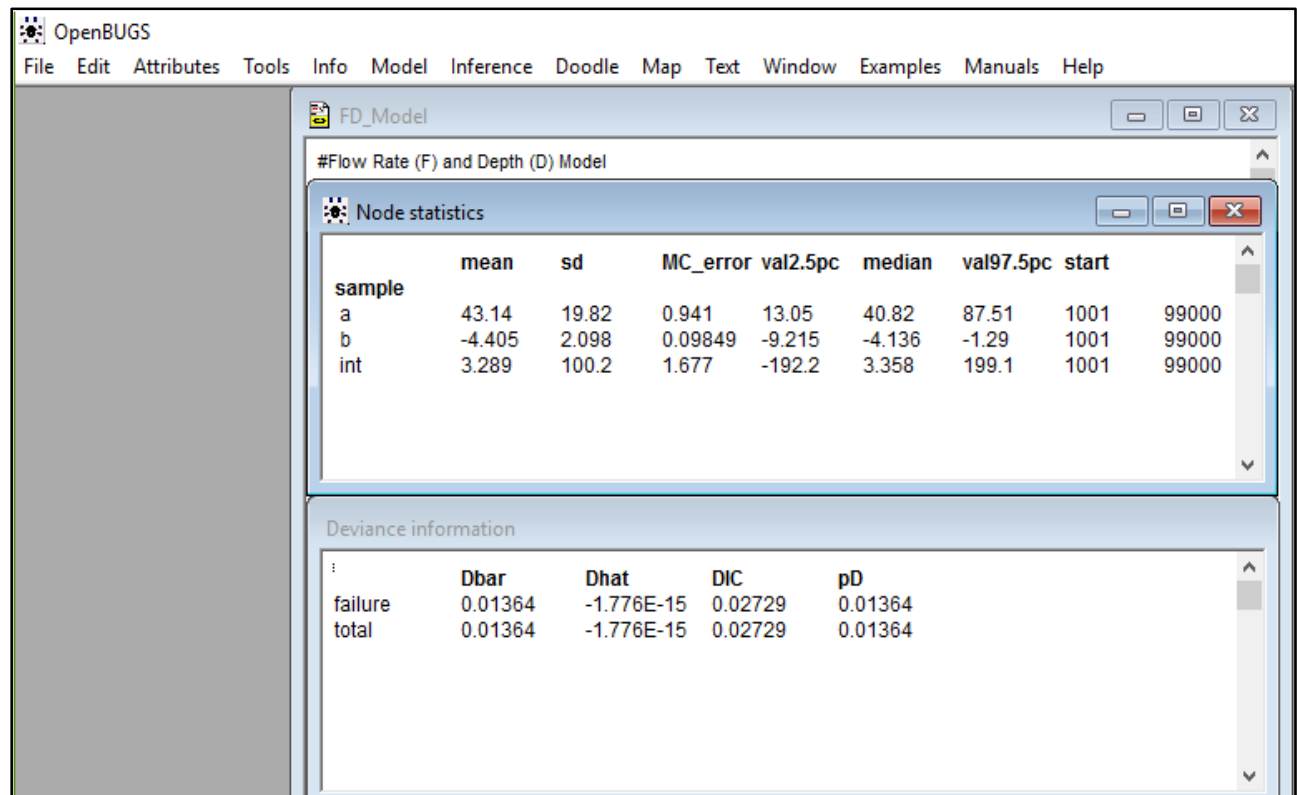
The screenshot shows the OpenBUGS interface for the 'T\_Model'. The title bar reads 'OpenBUGS' and the menu bar includes 'File', 'Edit', 'Attributes', 'Tools', 'Info', 'Model', 'Inference', 'Doodle', 'Map', 'Text', 'Window', 'Examples', 'Manuals', and 'Help'. The main window is titled 'T\_Model' and contains two panes. The top pane, titled '#Temperature (T) Model', displays 'Node statistics' for parameters 'c' and 'int'. The bottom pane, titled 'Deviance information', displays summary statistics for 'failure' and 'total'.

	mean	sd	MC_error	val2.5pc	median	val97.5pc	start	
sample								
c	0.09177	0.1763	0.009926	-0.1828	0.07187	0.4447	1001	99000
int	-6.659	11.82	0.6656	-30.46	-5.327	11.83	1001	99000

	Dbar	Dhat	DIC	pD
failure	11.29	10.22	12.36	1.07
total	11.29	10.22	12.36	1.07

### 4. Depth and Flow Model



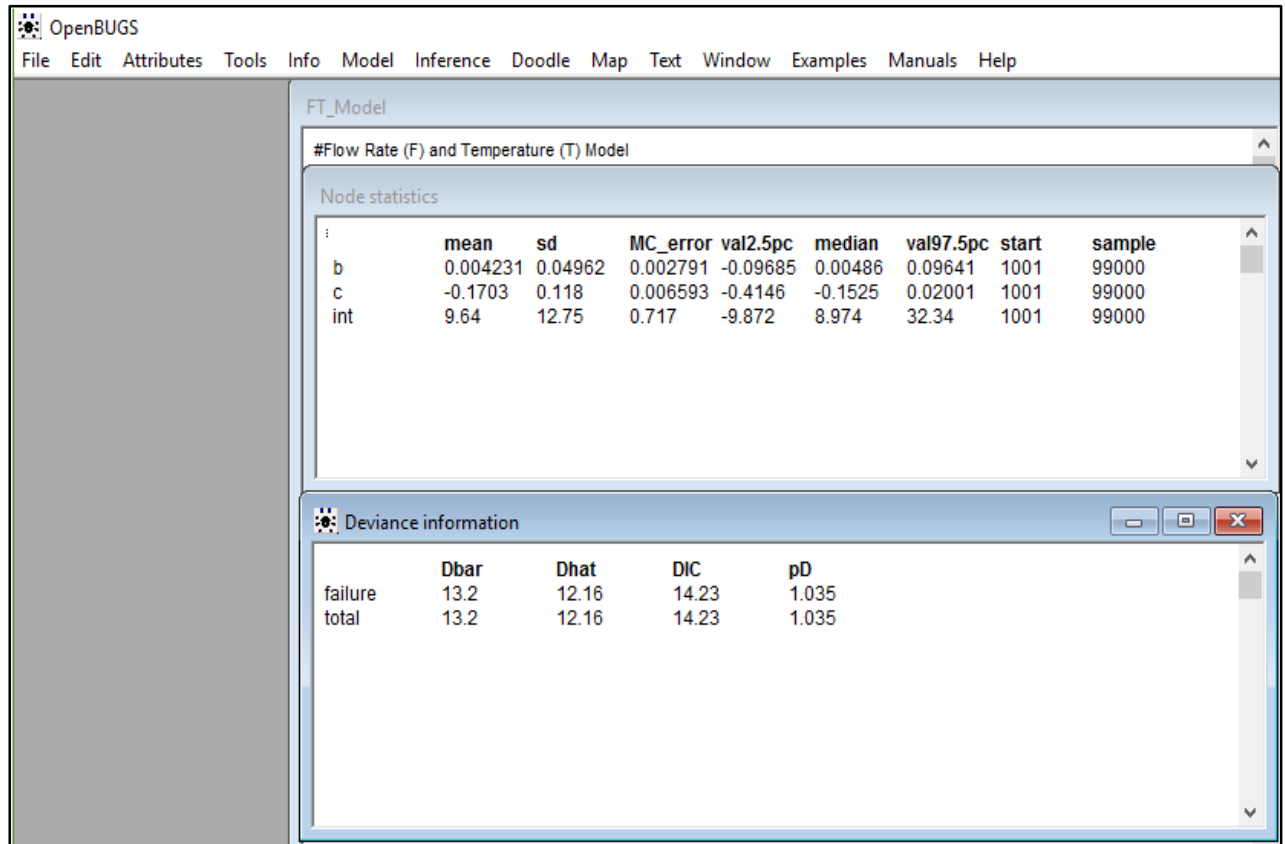
The screenshot shows the OpenBUGS interface for the 'FD\_Model'. The title bar reads 'OpenBUGS' and the menu bar includes 'File', 'Edit', 'Attributes', 'Tools', 'Info', 'Model', 'Inference', 'Doodle', 'Map', 'Text', 'Window', 'Examples', 'Manuals', and 'Help'. The main window is titled 'FD\_Model' and contains two panes. The top pane, titled '#Flow Rate (F) and Depth (D) Model', displays 'Node statistics' for parameters 'a', 'b', and 'int'. The bottom pane, titled 'Deviance information', displays summary statistics for 'failure' and 'total'.

	mean	sd	MC_error	val2.5pc	median	val97.5pc	start	
sample								
a	43.14	19.82	0.941	13.05	40.82	87.51	1001	99000
b	-4.405	2.098	0.09849	-9.215	-4.136	-1.29	1001	99000
int	3.289	100.2	1.677	-192.2	3.358	199.1	1001	99000

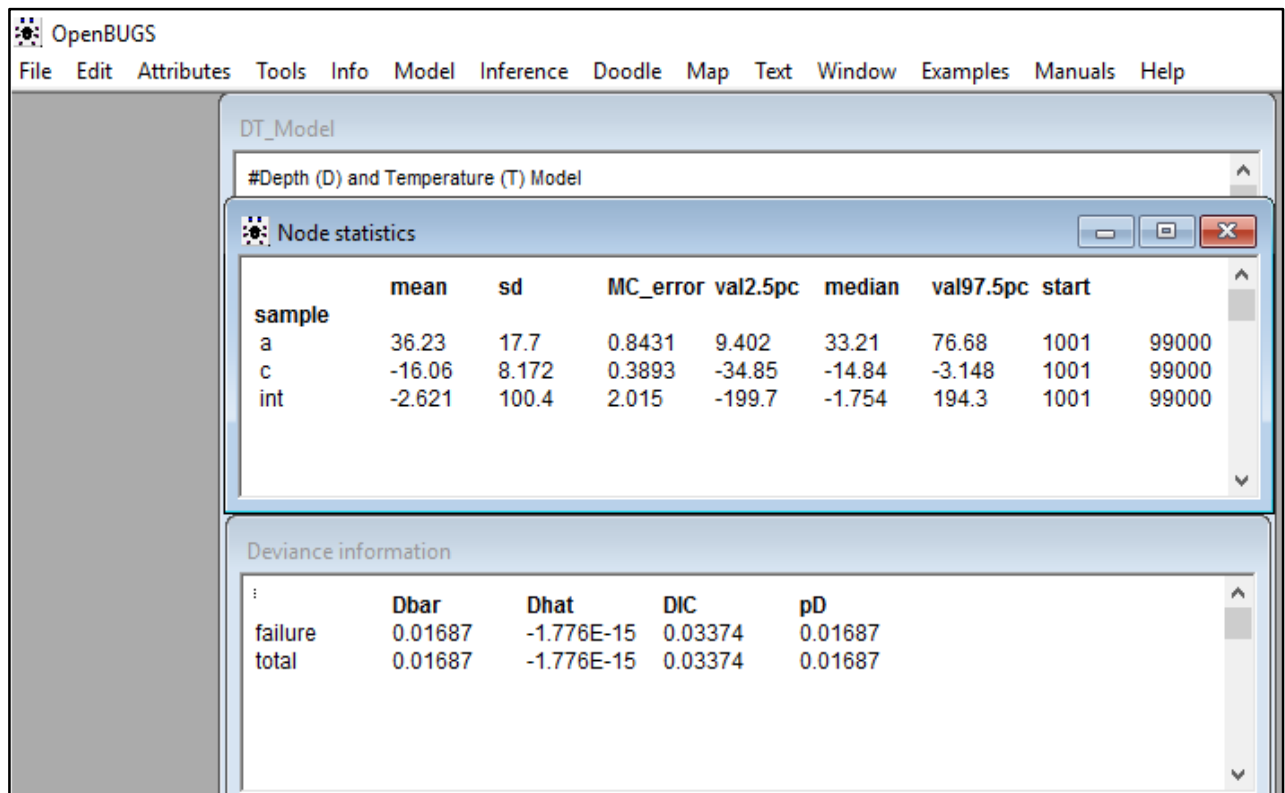
  

	Dbar	Dhat	DIC	pD
failure	0.01364	-1.776E-15	0.02729	0.01364
total	0.01364	-1.776E-15	0.02729	0.01364

## 5. Flow and Temperature Model



## 6. Depth and Temperature model





## 7. Depth, Flow and Temperature Model

The screenshot shows the OpenBUGS software interface. The main window displays the model name "FDT\_Model" and the description "#Flow Rate (F), Depth (D), and Temperature (T) Model". Below this, the "Node statistics" table provides summary data for parameters a, b, c, and the intercept (int). The "Deviance information" window is also open, showing the deviance components for failure and total data.

**Node statistics**

	mean	sd	MC_error	val2.5pc	median	val97.5pc	start	sample
a	42.37	19.44	0.9299	12.48	40.3	86.9	1001	99000
b	-7.109	7.631	0.4268	-20.79	-7.714	6.205	1001	99000
c	12.16	31.24	1.745	-44.48	16.69	66.62	1001	99000
int	5.653	98.89	1.694	-187.7	6.1	200.1	1001	99000

**Deviance information**

	Dbar	Dhat	DIC	pD
failure	0.01133	-1.776E-15	0.02266	0.01133
total	0.01133	-1.776E-15	0.02266	0.01133

# Appendix D

## 1. AND Gate (SN74LS08)

### SN5408, SN54LS08, SN54S08 SN7408, SN74LS08, SN74S08 QUADRUPL 2-INPUT POSITIVE-AND GATES

SDLS033 – DECEMBER 1983 – REVISED MARCH 1988

- Package Options Include Plastic "Small Outline" Packages, Ceramic Chip Carriers and Flat Packages, and Plastic and Ceramic DIPs

- Dependable Texas Instruments Quality and Reliability

#### description

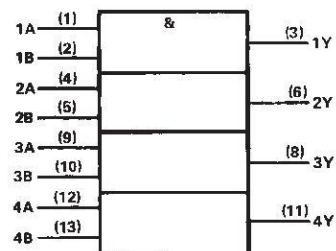
These devices contain four independent 2-input AND gates.

The SN5408, SN54LS08, and SN54S08 are characterized for operation over the full military temperature range of  $-55^{\circ}\text{C}$  to  $125^{\circ}\text{C}$ . The SN7408, SN74LS08 and SN74S08 are characterized for operation from  $0^{\circ}$  to  $70^{\circ}\text{C}$ .

FUNCTION TABLE (each gate)

INPUTS		OUTPUT
A	B	Y
H	H	H
L	X	L
X	L	L

#### logic symbol†

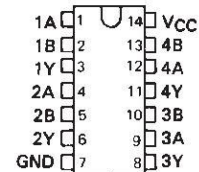


† This symbol is in accordance with ANSI/IEEE Std 91-1984 and IEC Publication 617-12.

Pin numbers shown are for D, J, N, and W packages.

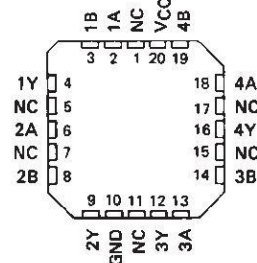
SN5408, SN54LS08, SN54S08 . . . J OR W PACKAGE  
SN7408 . . . J OR N PACKAGE  
SN74LS08, SN74S08 . . . D, J OR N PACKAGE

(TOP VIEW)



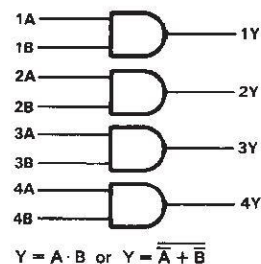
SN54LS08, SN54S08 . . . FK PACKAGE

(TOP VIEW)



NC—No internal connection

#### logic diagram (positive logic)



$$Y = A \cdot B \text{ or } Y = \overline{A + B}$$

## 2. OR Gate (SN74LS32)

SDLS100

### SN5432, SN54LS32, SN54S32, SN7432, SN74LS32, SN74S32 QUADRUPL 2-INPUT POSITIVE-OR GATES

DECEMBER 1983 - REVISED MARCH 1988

- Package Options Include Plastic "Small Outline" Packages, Ceramic Chip Carriers and Flat Packages, and Plastic and Ceramic DIPs
- Dependable Texas Instruments Quality and Reliability

#### description

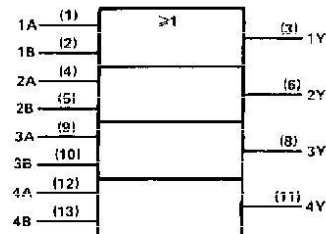
These devices contain four independent 2-input OR gates.

The SN5432, SN54LS32 and SN54S32 are characterized for operation over the full military range of  $-55^{\circ}\text{C}$  to  $125^{\circ}\text{C}$ . The SN7432, SN74LS32 and SN74S32 are characterized for operation from  $0^{\circ}\text{C}$  to  $70^{\circ}\text{C}$ .

FUNCTION TABLE (each gate)

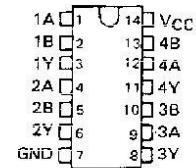
INPUTS		OUTPUT
A	B	Y
H	X	H
X	H	H
L	L	L

#### logic symbol†

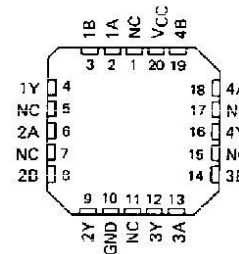


† This symbol is in accordance with ANSI/IEEE Std 91-1984 and IEC Publication 617-12.  
Pin numbers shown are for D, J, N, or W packages.

SN5432, SN54LS32, SN54S32 ... J OR W PACKAGE  
SN7432 ... N PACKAGE  
SN74LS32, SN74S32 ... D OR N PACKAGE  
(TOP VIEW)

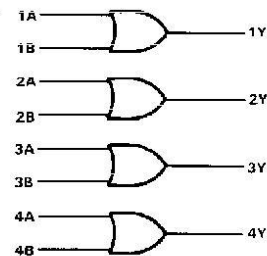


SN54LS32, SN54S32 ... FK PACKAGE  
(TOP VIEW)



NC - No internal connection

#### logic diagram



#### positive logic

$$Y = A + B \text{ or } Y = \overline{\overline{A} \cdot \overline{B}}$$

PRODUCTION DATA documents contain information current as of publication date. Products conform to specifications per the terms of Texas Instruments standard warranty. Production processing does not necessarily include testing of all parameters.

TEXAS  
INSTRUMENTS

POST OFFICE BOX 555012 • DALLAS, TEXAS 75265

## SN5404, SN54LS04, SN54S04, SN7404, SN74LS04, SN74S04 HEX INVERTERS

SDL5029C – DECEMBER 1983 – REVISED JANUARY 2004

**Dependable Texas Instruments Quality and Reliability**

**description/ordering information**

These devices contain six independent inverters.

**logic diagram (positive logic)**

$Y = \bar{A}$

**SN5404 ... J PACKAGE**  
**SN54LS04, SN54S04 ... J OR W PACKAGE**  
**SN7404, SN74S04 ... D, N, OR NS PACKAGE**  
**SN74LS04 ... D, DB, N, OR NS PACKAGE**  
**(TOP VIEW)**

**SN5404 ... W PACKAGE**  
**(TOP VIEW)**

**SN54LS04, SN54S04 ... FK PACKAGE**  
**(TOP VIEW)**

NC – No internal connection

**FUNCTION TABLE**  
(each inverter)

INPUT A	OUTPUT Y
H	L
L	H

Please be aware that an important notice concerning availability, standard warranty, and use in critical applications of Texas Instruments semiconductor products and disclaimers thereto appears at the end of this data sheet.

PRODUCTION DATA information is current as of publication date. Products conform to specifications per the terms of Texas Instruments standard warranty. Production processing does not necessarily include testing of all parameters.

**TEXAS  
INSTRUMENTS**

POST OFFICE BOX 655303 • DALLAS, TEXAS 75265

Copyright © 2004, Texas Instruments Incorporated  
 On products compliant to MIL-PRF-38535, all parameters are tested unless otherwise noted. On all other products, production processing does not necessarily include testing of all parameters.

## 4. 2:1 MUX (SN74LS157)

SDLS058

### SN54157, SN54LS157, SN54LS158, SN54S157, SN54S158, SN74157, SN74LS157, SN74LS158, SN74S157, SN74S158 QUADRUPLE 2-LINE TO 1-LINE DATA SELECTORS/MULTIPLEXERS

MARCH 1974 — REVISED MARCH 1988

- Buffered Inputs and Outputs
- Three Speed/Power Ranges Available

TYPES	TYPICAL AVERAGE PROPAGATION TIME	TYPICAL POWER DISSIPATION
'157	9 ns	150 mW
'LS157	9 ns	49 mW
'S157	5 ns	250 mW
'LS158	7 ns	24 mW
'S158	4 ns	195 mW

#### applications

- Expand Any Data Input Point
- Multiplex Dual Data Buses
- Generate Four Functions of Two Variables (One Variable Is Common)
- Source Programmable Counters

#### description

These monolithic data selectors/multiplexers contain inverters and drivers to supply full on-chip data selection to the four output gates. A separate strobe input is provided. A 4-bit word is selected from one of two sources and is routed to the four outputs. The '157, 'LS157, and 'S157 present true data whereas the 'LS158 and 'S158 present inverted data to minimize propagation delay time.

FUNCTION TABLE

STROBE G	SELECT A/B	INPUTS		OUTPUT Y	
		A	B	'157, 'LS157, 'S157	'LS158, 'S158
H	X	X	X	L	H
L	L	L	X	L	H
L	L	H	X	H	L
L	H	X	L	L	H
L	H	X	H	H	L

H = high level, L = low level, X = irrelevant

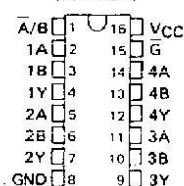
#### absolute maximum ratings over operating free-air temperature range (unless otherwise noted)

Supply voltage, $V_{CC}$ (See Note 1)	7 V
Input voltage: '157, 'S158	5.5 V
'LS157, 'LS158	7 V
Operating free-air temperature range: SN54'	-55°C to 125°C
SN74'	0°C to 70°C
Storage temperature range	-55°C to 150°C

NOTE 1: Voltage values are with respect to network ground terminal.

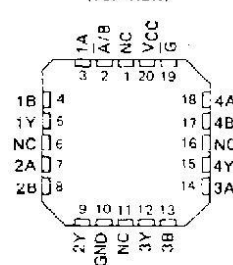
SN54157, SN54LS157, SN54S157,  
SN54LS158, SN54S158 ... J OR W PACKAGE  
SN74157 ... N PACKAGE  
SN74LS157, SN74S157,  
SN74LS158, SN74S158 ... D OR N PACKAGE

(TOP VIEW)



SN54LS157, SN54S157, SN54LS158,  
SN54S158 ... FK PACKAGE

(TOP VIEW)



NC = No internal connection

PRODUCTION DATA documents contain information current as of publication date. Products conform to specifications per the terms of Texas Instruments standard warranty. Production processing does not necessarily include testing of all parameters.

TEXAS  
INSTRUMENTS

POST OFFICE BOX 6555 DALLAS, TEXAS 75265

# Appendix E

## MTBF and Bathtub Curve

Note: The Bathtub curves for the logic components used are the same.

Refer: <http://www.ti.com/quality/docs/estimator.tsp>

### 1. AND Gate

	Early life failure rate	MTBF / FIT		Early life failure rate supporting data				MTBF / FIT supporting data						
Part number	ELFR-DPPM	MTBF	FIT	Conf level (%)	Test temp (°C)	Sample size	Fails	Usage temp (°C)	Conf level (%)	Activation energy (eV)	Test temp (°C)	Test duration (hours)	Sample size	Fails
SN74LS08N	61	1.38x 10 <sup>9</sup>	0.7	60	125	33359	1	55	60.0	0.7	125	1000	35687	1

#### Definition of Table Terminology

Part #:The TI orderable part number

ELFR: Early Life Failure Rate

DPPM: Defective Parts Per Million

MTBF: Mean Time Between Failures

FIT: Failures-in-Time. The number of failures per 1E9 device-hours

Conf level %: Statistical confidence level

Test temp (°C): Temperature at which the stress test is performed

Sample size: Sample size is how many units were tested and would be based on the normalized value for duration

Fails: The number of failures per test

Usage temp (°C): Estimated usage temperature

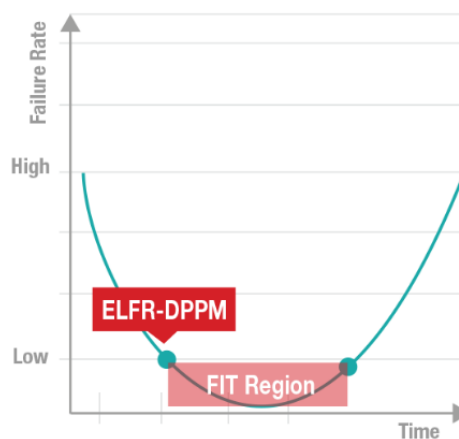
Activation energy (eV): Energy in electron volts (eV) for a particular process to occur

Test duration (hrs): Test duration is a field that comes from the qualification testing of a product. Since more than one test is conducted and the duration varies, this field will be normalized based on calculations using temp, quantity and fails. This value would be equivalent unit hours.

NA: Not Applicable

TBD: To Be Determined

### Bathtub Curve



ELFR/DPPM - Early Life Failure  
MTBF/FIT - Long Term Reliability

## 2. OR Gate

	Early life failure rate	MTBF / FIT		Early life failure rate supporting data				MTBF / FIT supporting data						
Part number	ELFR-DPPM	MTBF	FIT	Conf level (%)	Test temp (°C)	Sample size	Fails	Usage temp (°C)	Conf level (%)	Activation energy (eV)	Test temp (°C)	Test duration (hours)	Sample size	Fails
SN74LS32N	61	1.38x 10 <sup>9</sup>	0.7	60	125	33359	1	55	60.0	0.7	125	1000	35687	1

## 3. NOT Gate

	Early life failure rate	MTBF / FIT		Early life failure rate supporting data				MTBF / FIT supporting data						
Part number	ELFR-DPPM	MTBF	FIT	Conf level (%)	Test temp (°C)	Sample size	Fails	Usage temp (°C)	Conf level (%)	Activation energy (eV)	Test temp (°C)	Test duration (hours)	Sample size	Fails
SN74LS04N	61	1.38x 10 <sup>9</sup>	0.7	60	125	33359	1	55	60.0	0.7	125	1000	35687	1

## 4. 2:1 MUX

	Early life failure rate	MTBF / FIT		Early life failure rate supporting data				MTBF / FIT supporting data						
Part number	ELFR-DPPM	MTBF	FIT	Conf level (%)	Test temp (°C)	Sample size	Fails	Usage temp (°C)	Conf level (%)	Activation energy (eV)	Test temp (°C)	Test duration (hours)	Sample size	Fails
SN74LS157N	61	1.38x 10 <sup>9</sup>	0.7	60	125	33359	1	55	60.0	0.7	125	1000	35687	1